AMERICAN OIL COMPANY

AD624092

RESEARCH AND DEVELOPMENT

DEPARTMENT

THE FO RADICAL
AND
HIGH PRESSURE REACTIONS OF N_2F_2

ELEVENTH QUARTER REPORT
NOVEMBER, 1965

M65-265

PREPARED FOR
UNITED STATES ARMY RESEARCH OFFICE (DURHAM)
DURHAM, NORTH CAROLINA

THE FO RADICAL

AND

PRESSURE REACTIONS OF N_2F_2

Eleventh Quarter Report

November, 1965

M65-265

Prepared for

United States Army Research Office (Durham)

Durham, North Carolina

FOREWORD

This report was prepared by the American Oil Company under Contract DA-31-124-ARO(D)-78. The program was initiated under ARPA Order 402, Task 5, ARPA Program Code 3910, ARO-D Project 4135C.

This eleventh quarter project report covers the period August 1, 1965 to November 1, 1965. Scientists working on this project are A. Zletz, Project Leader, and E. M. Banas, W. J. Cerveny, J. A. Donohue, R. D. Hites, R. R. Hopkins, J. D. McCollum, A. G. Nerheim, R. L. Stoffer, and R. W. Vander Haar.

This is a progress report and the results presented should be regarded as tentative.

NOTICE

ABSTRACT

Efforts to generate gaseous OF centered upon flash photolysis
of CF_3COOF at low temperature. Two transient phenomena were found: at
77°K violet phosphorescence from the solid and at higher temperature two
diffuse absorption bands from the gas. Because the phosphorescence is
observed from the solid of several fluorocarbonyl compounds, the phosphor
is likely an impurity excited by energy transfer from the host lattice.
The transient absorption spectrum is not produced from the other carbonyl
compounds nor from products of CF_3COOF. Therefore, the transient is
related to CF_3COOF photolysis. Attempts to identify the transient are
in progress.

Mass spectrometric search for OF from OF_2 and other hypofluorites
was impeded because of poor mass resolution by the MS-10 mass spectrometer.
This condition was corrected and decomposition studies are in progress.

For electrolytic generation of OF_2 from wet HF, ohmic overvoltage
at the nickel anode was determined by both potential decay and superim-
posed square wave. The ohmic overvoltage at normal electrolysis condi-
tions was surprisingly low (0.25 to 0.40 v. at 4.8 v. anode). Also,
changes in product yield did not give rise to changes in the ohmic over-
voltage. The origin of product yield changes at the anode will be sought
by other electrochemical methods.

Work continued on the structure of N_2F_2 complexes. Solutions
of N_2F_2 in SbF_5, blue when fresh but rapidly fading to yellow, were examined
by electron paramagnetic resonance to determine if the color arises from
free radicals. An EPR spectrum of the yellow solution could be resolved

into two separate spectra. The sixteen-line spectrum is consistent with the SbF_5^- radical while the five-line spectrum arises from an N_2 containing radical of as yet unknown composition.

TABLE OF CONTENTS

LIST OF FIGURES

I. INTRODUCTION

This study involves two areas of inorganic fluorine chemistry--
the OF radical and the chemistry of difluorodiazine (N_2F_2). Both sub-
stances are potential intermediates for synthesis of new fluorine com-
pounds.

Program objectives are:

1. Study the existence of the OF radical produced by photochemical
   and electrochemical techniques.

2. Investigate the behavior of N_2F_2, both alone and in the presence
   of other inorganic NF reagents, with and without catalysts, at
   10^4 atm and higher.

The work carried out during this quarter is presented in three parts:
fluid-phase formation and detection of OF, electrolysis of wet hydrogen
fluoride, and high-pressure reactions of N_2F_2.

II. THE OF RADICAL: FORMATION AND DETECTION IN FLUID PHASES

Introduction

Although OF has now been identified by elegant infrared methods in low-temperature matrix experiments[1], the radical has so far proven too unstable or too reactive to be detected spectroscopically in the gas phase. As part of our program on flash photolysis of hypofluorites[2,3,4], we have now examined trifluoroacetyl hypofluorite, $CF_3\overset{O}{\overset{\parallel}{C}}OF$, both gaseous and in solution at low temperature. Thermolytic studies[5] have indicated that the $CF_3\overset{O}{\overset{\parallel}{C}}O-F$ is the weakest bond to thermal dissociation, but flash photoexcitation can perhaps result in $CF_3\overset{O}{\overset{\parallel}{C}}-OF$ bond cleavage. A high photolytic rate of formation coupled with reduction of uni- and bi-molecular decay rates by low-temperature operation should favor accumulation of OF for optical spectroscopic detection. This report describes photolytic intermediates and products found in our survey of $CF_3\overset{O}{\overset{\parallel}{C}}OF$ photolysis.

Mass spectrometric detection is more sensitive than optical spectroscopy, and we are preparing to use this method to seek OF from flow thermolyses and photolyses.[2] However, instrument difficulties have delayed its use to date.

Preparation of $CF_3\overset{O}{\overset{\parallel}{C}}OF$

The hypofluorite was prepared by fluorination of CF_3COOH[6,7]; fresh batches were made for each photolytic experiment.

$$CF_3COOH + F_2 \xrightarrow{H_2O} CF_3\overset{O}{\overset{\parallel}{C}}OF + HF$$
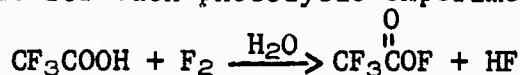
The product, purified by fractionation and stripping, decomposed (spark or thermal) to give roughly a twofold pressure rise, corresponding to CO_2 + CF_4 formation. Infrared analysis showed that the final product contained small amounts of CF_3COOH, SiF_4, and CF_2O, in addition to CF_3COOF (1860 cm^{-1}, 1070 cm^{-1}) and the CO_2 + CF_4 decomposition products. Infrared frequencies for the hypofluorite were assigned because they disappeared as the hypofluorite decomposed, and because the hypsochromic shift in stretching frequencies is about that predicted for carboxylic double and single bonds when H is replaced by F. Stewart and Cady have reported[5] thermal decomposition of CF_3COOF at room temperature by a chain reaction second order in hypofluorite. We found that the hypofluorite, at an initial pressure of about 10 torr, disappeared with an 30-sec. half-life, about three times that estimated from the published specific rate. The appearance of CF_2O as a primary decomposition product suggests oxygen contamination in our reaction vessel and infrared cell—both inhibition of the decomposition and CF_2O formation due to oxygen addition were noted by Stewart and Cady. However, our photolysis experiments were carried out in vacuum-tight cells and handling equipment and therefore could not have been contaminated with oxygen.

Flash Photolysis of $CF_3\overset{O}{\overset{\|}{C}}OF$

Because low-temperature solutions afford a relatively easy experimental approach to low-temperature flash photolysis, we attempted to prepare solutions of $CF_3\overset{O}{\overset{\|}{C}}OF$ in liquid NF_3 (b.p. 149°K). As with other hypofluorites (excepting FOF and FOOF)[3,4], the compound was too insoluble to allow examination by absorption spectroscopy.

Low-temperature gas phase flash photolyses were carried out in vacuum-jacketed gas cells containing an internal coil which could be cooled by liquid nitrogen or other coolants. For survey experiments, we used this experimental pattern:

A) A known amount of CF_3COOF, purified and checked by infrared on an aliquot, was condensed ($77°K$) as a white solid on the cooling coil of the gas cell. An absorption spectroflash of this cell taken during a photolytic flash was used as a reference for further absorption spectra since no gas was present in the cell ($p < 0.1$ torr).

B) The coolant was flushed from the coil and the contents were allowed to warm. Coil temperature was followed by a thermocouple--the internal gas temperature was always slightly less than that of the coil. The solid melted and vaporized as it warmed. At intervals, the cell contents were photoflashed; flash absorption spectra were taken during the photoflash to reveal any transient absorptions accompanying photolysis, and after the photoflash, to give the absorption spectra of photoproducts. The latter spectrogram includes thermal products, but we expect thermal reactions to be slow below $250°K$.

C) After the cell had warmed completely (1-2 hours), ultimate products were determined by infrared.

From flash photolysis of $CF_3\overset{\text{O}}{\overset{\text{\tiny ll}}{C}}OF$ we found two transient phenomena: first, a bright violet phosphorescence in the solid on the

cooling coil; and second, at higher temperatures, two diffuse absorption bands of a transient in the gas phase.

The violet phosphorescence (about 3-sec. life time) was present only in solid CF_3COOF and disappeared at the melting point (about $160°K$). Following total volatilization of the sample, the phosphorescence could be obtained again if the sample or its decomposition products were recondensed and photoflashed. Other solid fluoro-carbonyl compounds when photoflashed gave qualitatively the same phosphorescence. Phosphorescence intensity increased in the order $CF_2O <$ $CF_3COOH \sim CF_3COOF < CF_3COCF_3$. Because the absorption edges for these compounds move to the visible in the same order, the fraction of photo-excitation from the photoflash ("white" light from 2000-7000 Å tailing off below 2000 Å) increases in this same pattern. Since the same phosphorescence is produced from these sources, the phosphor most likely is an impurity which is excited by energy transfer from the host lattice. The phosphorescence does not seem to be associated with primary photolysis of the hypofluorite.

The transient absorption spectrum, on the other hand, does appear to be associated with CF_3COOF photolysis. Flash photolysis with the cell cooled below $200°K$ shows no short-lived absorption. However, the partial pressure of CF_3COOF (b.p. $251°K$) is low in this region, so little photolytic light is absorbed. (We have not yet obtained a good absorption spectrum of CF_3COOF; however, its strong bands, like those of CF_3COCH, appear to lie in the far ultraviolet with only tailing into

the quartz ultraviolet.) Between 200°K and 250°K, the photoflash is attended by the clear appearance of two band maxima at $258m_\mu$ and $255\ m_\mu$. Further bands may appear at $248\ m_\mu$ and in the $260-270\ m_\mu$ interval, but these regions are overlaid by other absorptions and are quite tentative. The new bands are not generated from any of the other carbonyl derivatives and cannot be produced from products present after CF_3COOF has been completely decomposed. Therefore, the transient seems clearly related to CF_3COOF photolysis; however, assignment has not been made. Carriers with known spectra in this region, as CF_2, need to be ruled out. Better defined spectra, kinetic spectroscopic measurements of the transient life time, and further correlation experiments with potential transient sources are planned to aid assignment.

Absorption Spectra of Flash Photolysis Products from $CF_3\overset{\overset{\displaystyle O}{\displaystyle \|}}{C}OF$

At low temperature (77°K), the gas cell was transparent in the ultraviolet. As the coil warmed, flash spectra following flash photolyses of the cell contents showed new diffuse absorption bands due to decomposition products from CF_3COOF. The results are summarized as follows:

Approximate Temperature[a], °K	State	Gaseous Absorption Spectrum, $_{max}$ in m_μ (absorbance)
77	White solid	Nil
150	White solid	Onset of absorption at short wavelength edge.
200	Liquid	a) 245, 270 (0.04) b) 280 (0.003) c) 296 (0.04), 314 d) 368 (0.16) (c)
250	Trace of liquid	a) 245 270 (0.05) b) 280 (0.10) c) 296 (0.10), 314 d) 368 (0.30) (c)

a) Temperature of internal coil-cell temperature slightly lower.
b) Condensate on coil.
c) Transient appears during photoflash--see preceding section.

Increased absorption below 250 m_μ is expected as the cell

warms and the CF_3COOF vaporizes. By the time the cell temperature

reaches 200°K the contents have been exposed to 3 to 4 photoflashes.

New bands, shown in the table, reflect products from photolysis of the

gas and, to some extent, of the solid remaining on the cooling coil.

New bands fall into a pattern of four groups which seem to change in

intensity together. The table lists absorbances for a band in each

group determined from densitometry of flash spectra. Bands in the near

u.v. appear much like carbonyl bands--the group "C" in particular

resemble CF_3COCF_3.[7] It is then tempting to consider a diketone such

as $CF_3COCOCF_3$ for the higher band at 368 m_μ, but no identification has

been made yet; polyoxygen difluorides are also possible absorbers. The

sharply rising band near 280 mμ falls where F_2 absorbs and may represent a primary or secondary photochemical formation of the element. When cells are recooled following a sequence of flash photolysis with warming, these absorbances are largely eliminated. The 280 mμ band decreases more slowly, as would be expected if it were due to F_2, which will not condense at 77°K but must disappear by reaction.

After warming to room temperature and standing for 1-2 hours, the products (IR) are largely CO_2, CF_4, CF_2O, HF; SiF_4 from reaction with the cell is also found. No hypofluorite remains.

These survey experiments indicate products consistent with photolysis of CF_3COOF at the carbonyl group are formed. We plan now to conduct flash photolysis at 200°K with provision for both IR and mass spectrometric analysis of products. We also seek to assign the product ultraviolet spectra by correlation with known compounds.

Mass Spectrometrometric Detection

For some time the MS-10 mass spectrometer has been giving poor mass resolution and irreproducible peak heights. The ratio of peaks is necessary in our study to help show the molecular species from which the mass peak is derived. Instability in peak heights introduces intolerable errors in peak ratio measurements.

Origin for the difficulty was first sought in the associated electronics and then in the mass analyzer element. No sources of difficulty were found in extensive searches for possible electronic contributions. Repeated cleaning of the working parts in the mass spectrometer

gave no permanent improvement. The offending part was finally identi-
fied as the supporting frame piece bearing the 90° ion beam-defining
slit (α-slit). This was done by substituting parts from a new MS-10
analyzer. Normal MS-10 operation was restored after the defective
piece had been etched strongly with hydrochloric acid and polished.

A likely cause of the instability is a semiconducting layer
on the front metal around the α-slit. Slower than normal dissipation
of charges (resulting from impingement of ion beams on the surface)
could cause spreading of ion beams, which would in turn cause loss in
mass resolution and ion beam intensity. Whether attack by OF_2 was
responsible for the difficulty may be revealed when we resume studies
with OF_2. We can now return to the thermolysis study of OF_2 and examine
OF/OF_2 (35/54) m/e ratio with changing temperature and the ionization
efficiency curves for the two ions.

Experimental

CF_2O, CF_3COCF_3 (Penninsular), NF_3 (Air Products and Chemicals)
and CF_3COOH (Allied Chemical) were chemically pure compounds used as
received.

CF_3COOF was prepared according to the receipe of Cady and
Kellog[4]--CF_3COOH, F_2, and H_2O, each in an N_2 carrier gas stream, were
allowed to react in polyethylene vessels. The effluent stream was passed
through successively colder traps to remove unconverted reactants.
Finally, products were condensed (77°K) in a trap attached to a vacuum
line and pumped to remove F_2 and N_2.

Products were transferred by vacuum line methods either to infrared or to photolysis cells. Infrared cells (5 cm path) were made of Teflon with AgCl windows.

Vacuum-jacketed silica cells for flash photolysis of low-temperature solutions and gases were described in previous reports.[2] Low-temperature solutions were prepared by condensing (77°K) first CF_3COOF and then NF_3 solvent into the cell to make up the desired liquid volume. With the gas cell, samples were condensed on an internal cooling coil filled with liquid nitrogen. Flash photolytic and flash spectroscopic techniques were described earlier.[2]

Program

Since product spectra from these survey experiments are consistent with compounds produced by photocleavage of bonds adjacent to the carbonyl group in $CF_3\overset{O}{\overset{\|}{C}}OF$, our detection of a photo-transient spectrum from this compound is particularly interesting. We therefore plan further experiments to seek to identify the photo-transient. These include: efforts to brighten the transient spectrum; kinetic spectroscopic measurements of the lifetime and of quenching of the transient; and correlation experiments with other compounds which might give fragments in common with those from $CF_3\overset{O}{\overset{\|}{C}}OF$. Using mass spectrometry, we shall resume study of OF_2 thermolysis and photolysis. Hypofluorites will also be examined as possible sources for OF. These experiments will complete our projected work on optical detection of OF for this year.

III. THE OF RADICAL: ELECTROLYSIS IN WET HF

The OF radical may be an intermediate in the formation of OF_2 during the electrolysis of wet HF. Our study of this electrolysis has a two-fold objective: (1) formulate a reaction mechanism on the basis of operating conditions, electrolyte composition, and product distribution, and (2) use electrochemical measurements to test and supplement this mechanism and to attempt to detect reaction intermediates.

During the electrolysis, gaseous products are swept out by helium and are sampled for gas chromatography. Changing product yields are readily seen by a rapid gas chromatographic analysis of the gaseous products (O_2, O_3, OF_2, H_2).

Water concentration was found to be important to OF_2 yield, but even careful control of water concentration was not sufficient to maintain constant OF_2 yield. However, periodic interruption of the electrolysis gave constant OF_2 yields over several hours. We believe interrupted operation gives constant yield by maintaining a steady-state composition of the anode surface film.

Studies at constant cell voltage showed the effects of H_2O and KF concentrations, interruption rate, temperature, and mercury impurity on the OF_2 yields. Later, when the Hg/Hg_2F_2 reference electrode was sufficiently developed for use in wet HF, the effects of anodic voltage on OF_2 yields wer died.

During this quarter changing the anode voltage-drop during interruption was found to have a small effect on yield. Components of

the anodic potential were determined by a decay method and a super-
imposed square wave method for resistance measurement seeking clues to
electrode mechanisms. The ohmic overvoltage (mostly due to anodic film
resistance) is surprisingly small, while activation overvoltage is at
least as great as the limiting potential (i.e., E_O + Nernst terms) as
determined by decay measurements.

The action of gaseous oxygen atoms on NiF_2 was examined for
clues to OF_2 formation. No OF_2 was observed.

Experimental

The main electrolysis cell[2a] (now with an anode area of
2.5 cm^2 and a cathode area of 10 cm^2), analytical techniques[2b], and
the reference electrode[4a] have been described. Ohmic overvoltage was
determined by two methods: potential decay and superimposed square
wave. Potential decay was also used to evaluate activation overvoltage
and the limiting potential.

Potential Decay--The components are those described previ-
ously[4b] for chronopotentiometry, : they have been rearranged to give
decay curves. This is shown in Figure 1, which also shows the timer
for interrupted operation.[2a]

In normal operation, switch S_1 is set to the automatic timer,
while switch S_3 is set to position 2 to include relay R_1 but not R_2.
During interrupted operation the potentiostatic control voltage is
switched by the timer from CV No. 1 to CV No. 2 for 1 sec. every 120
sec. The potential drop during interruption is controlled by CV No. 2.

FIGURE 1
POTENTIAL DECAY
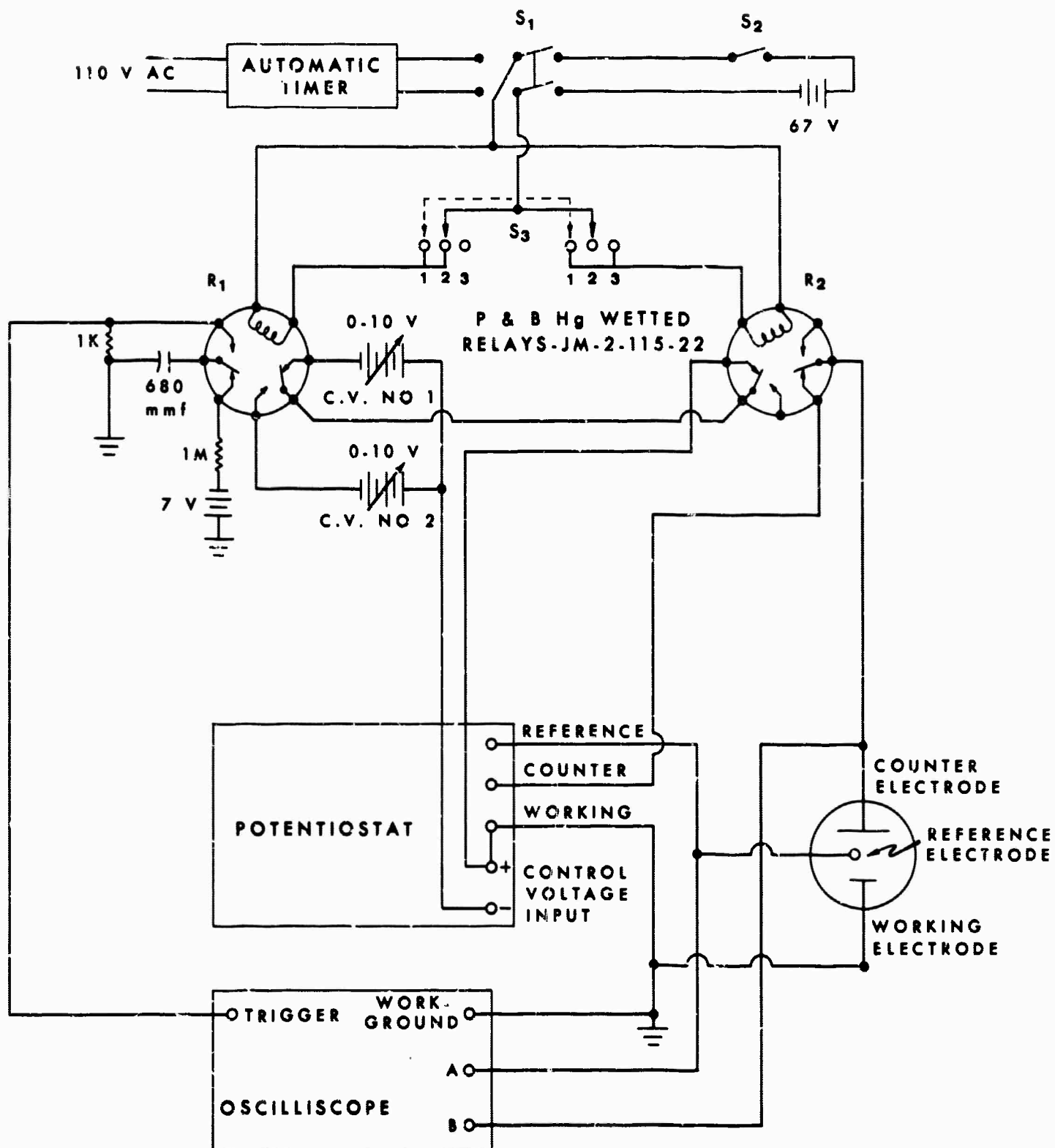
With switch S_1 still set for normal operation, the oscilloscope is triggered during the interruption, but the AC from the timer produces noise on the oscilloscope. Therefore, a D.C.-operated trigger for decay was incorporated. When a decay curve is desired, switch S_1 is shifted to the 67 v. battery position, and S_3 is set to position 1 to activate both relay R_1 and relay R_2. Then switch S_2 is closed, disconnecting the potentiostat from the electrolysis cell and triggering the oscilloscope.

Potential decay was also used to measure ohmic overvoltage during continuous electrolysis. The automatic timer was not used and S_3 was at position 2. To obtain a decay curve, the above procedure is repeated; namely, S_1 is set to the 67 v. battery position, S_3 is set to position 1, and S_2 is closed.

The value of the ohmic overvoltage (η_R) can be determined from the break in the first 0.1 millisecond of the decay curve (Figure 2). The limiting potential ($E\infty$) is determined when the decay curve levels off. The optimum time for this measurement has not yet been determined, but it is on the order of minutes. Combined activation and concentration overvoltage ($\eta_A + \eta_C$) is calculated by difference.

Superimposed Square Wave--A Hewlett-Packard square-wave generator (211A) at 500 pulses per second was used. However when it was superimposed on the potentiostatically controlled cell, the potentiostat responded and distorted the square wave. This was avoided by switching from potentiostatic to galvanostatic operation for the measurement. The components and arrangement are shown in Figure 3.
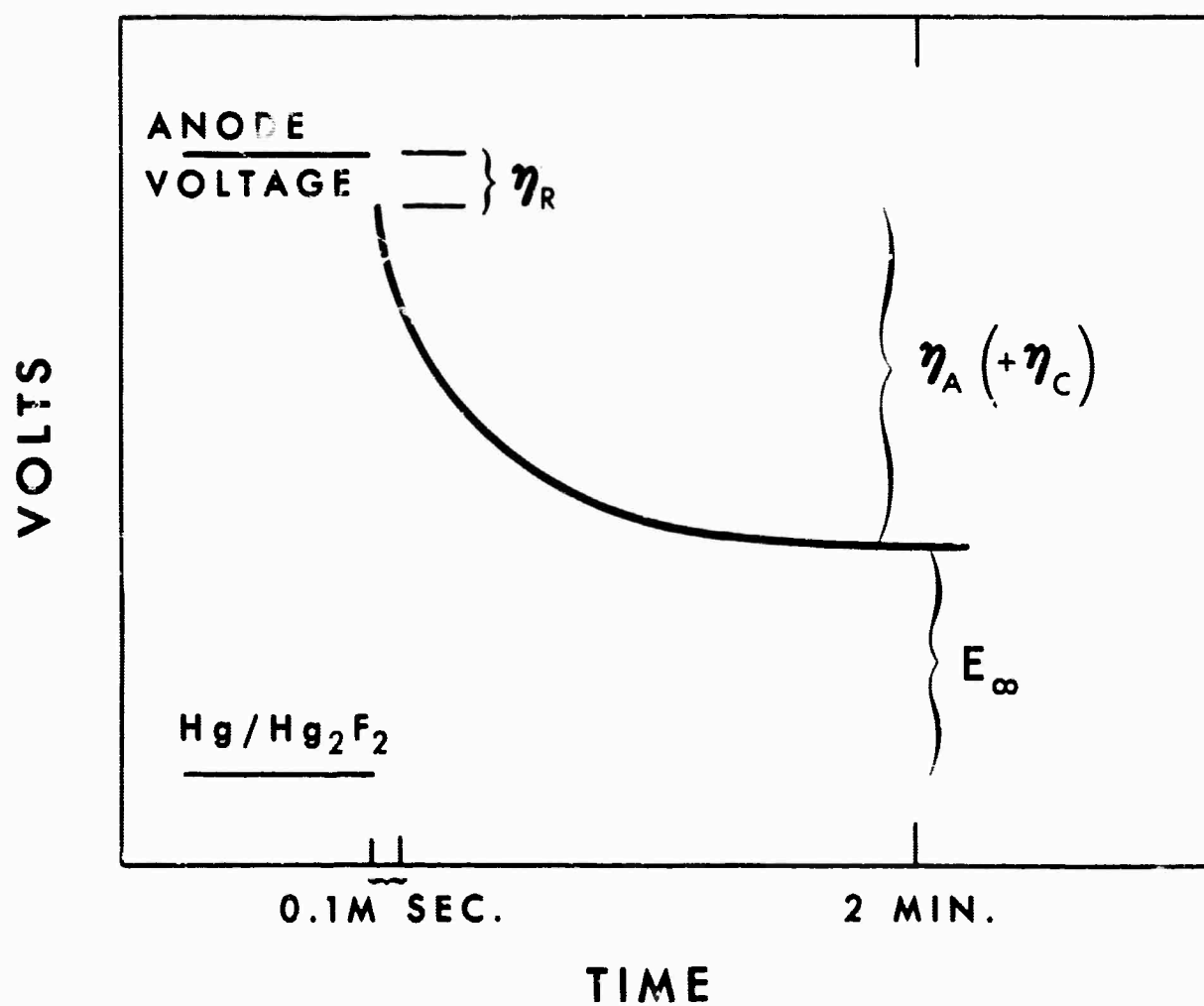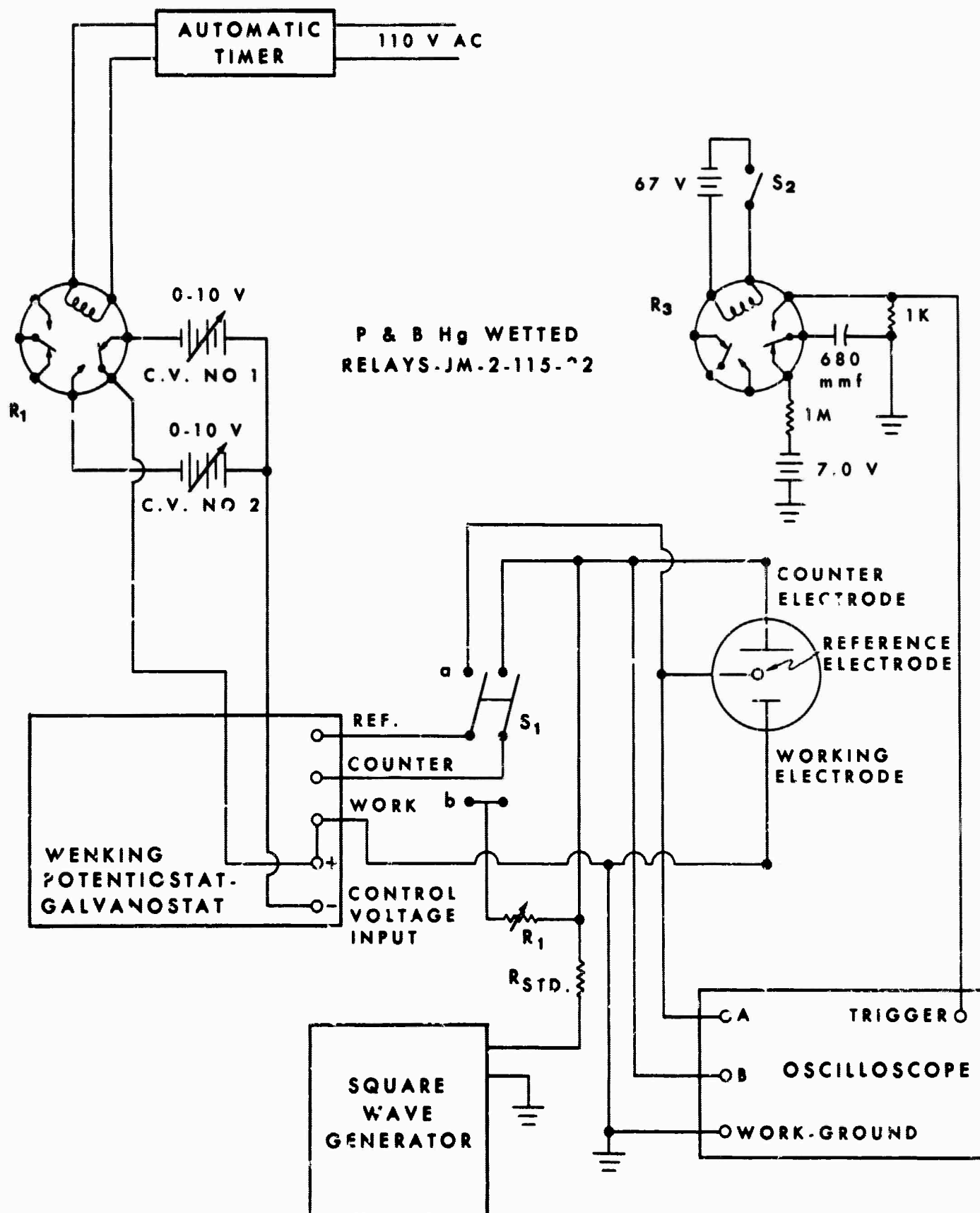
FIGURE 2

SAMPLE DECAY CURVE

FIGURE 3
SUPERIMPOSED SQUARE WAVE

In normal operation (interrupted-potentiostatic control), switch S_1 is at position a (Figure 3). To permit a measurement, switch S_1 is reversed to position b. This joins the counter and reference circuits from the Wenking to the counter electrode via a variable resistance (R_1) to give galvanostatic operation. By proper adjustment of R_1 and the control voltage (CV No. 1 and 2), the cell voltage and current can be kept approximately the same as during potentiostatic operation. This switching and adjusting takes 15-20 seconds and therefore is a longer interruption than normal (1 sec.).

The square-wave output and R std. are adjusted to give a known current at 500 cycles/sec. when superimposed on the electrolysis cell. The IR drop of this signal can be determined from its oscilloscope pattern. Because stray 60-cycle AC distorts the 500-cycle signal, the signal cannot be displayed continuously. Instead, the scope is triggered to give a single display by closing S_2 which activates relay R_3. From the voltage drop found on this display and the known square-wave current, an electrode resistance can be calculated. This resistance and the known DC current give the ohmic overvoltage η_R.

Results

Interrupted Voltage Drop--The effects of impressed voltage during interruption are shown in Figure 4. In the range of 1.5 to 3.5 anode voltage during interruption there is no effect on yields. The voltage drop is in this range when no voltage is imposed during interruption and confirms an assumption made in our last report when studying

FIGURE 4

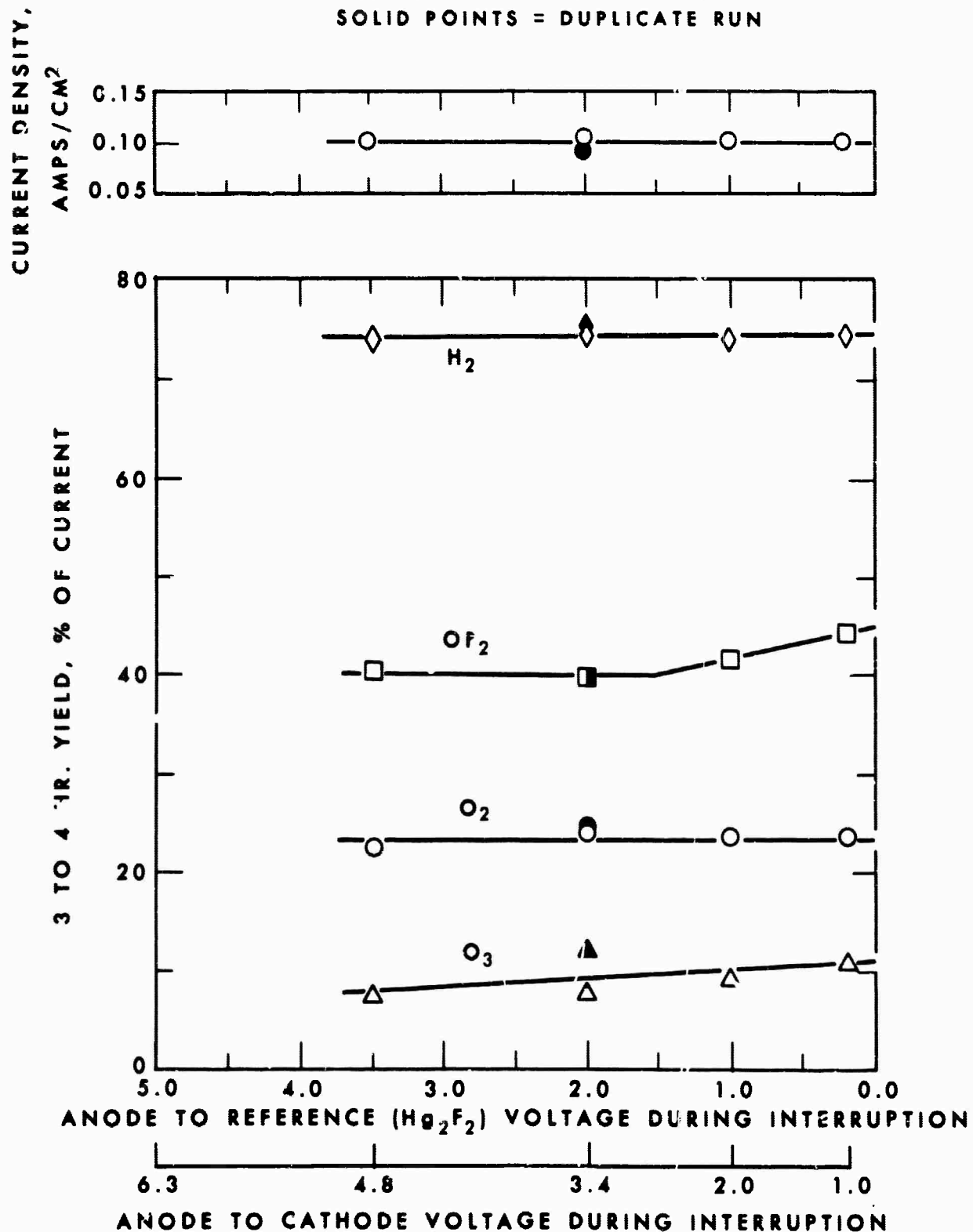## EFFECT OF VOLTAGE DROP DURING INTERRUPTION

CONDITIONS:
  $H_2O \approx 0.67$ MOLE %
  $KF \approx 1.0$ MOLE %
  TEMP.$=1.2°C$
  INTERRUPTION RATE=1 SEC./120 SEC.
  SOLID POINTS = DUPLICATE RUN

4c

effect of cell voltage.[4c] However, at large voltage drops the OF_2 yield appears to be increasing slightly.

Ohmic Overvoltage--The ohmic overvoltage (η_R) of both electrodes determined by the two methods are shown in Figure 5 as a function of current density. The cathode show values of less than 0.1 v. by both methods, and is thus a negligible factor with cell voltages that generally are 6.0 v. or more.

The anode values are also quite small. At normal cell conditions (0.1 amp/cm^2; cell voltage = 6.2; anode voltage = 4.8) the potential decay method showed 0.25 v. while the square wave method gave ~0.40 v. The discrepancies between the two methods are possibly due to effects of the alternating square wave on the electrode surface; as both measurements show low η_R, no attempt was made at this time to resolve the difference.

The η_R of continuous operation was also found to be quite low, in fact even lower than interrupted operation. Since determination of η_R by potential decay requires interrupting the current, repeated determinations approach the interruption values. However, this is due to changes in the current density with interruption rather than any great change in η_R.

The same values of η_R were obtained regardless of whether current density was progressively increased or decreased (Figure 5). However, the yield of OF_2 was not constant and Figure 6 shows a drop in OF_2 yield as current density was decreased. The effect was observed
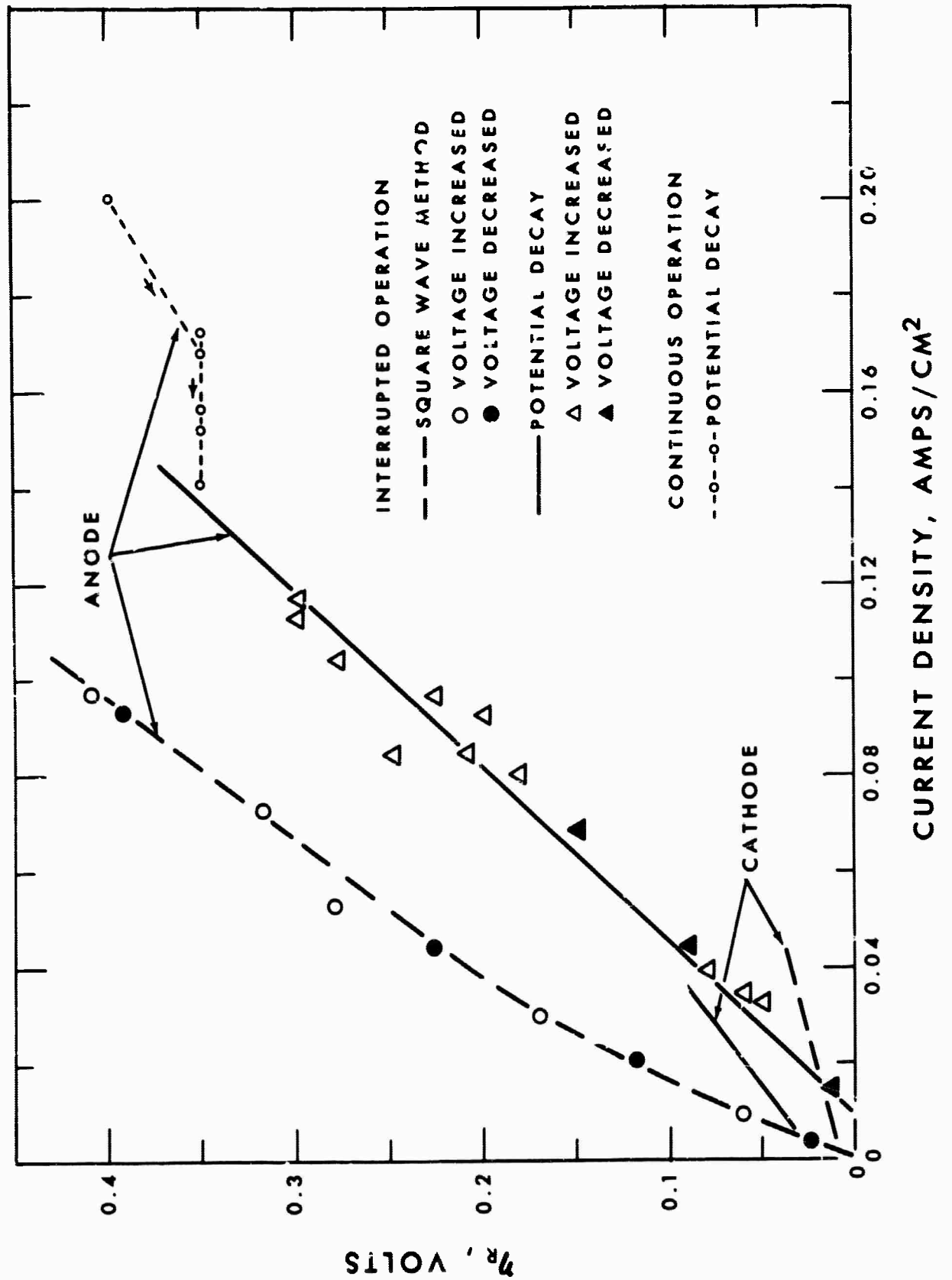
FIGURE 5

OHMIC OVERVOLTAGE

CURRENT DENSITY, AMPS/CM²

FIGURE 6

OF$_2$ YIELD VARIATION WHILE
MEASURING OHMIC OVERVOLTAGE

CELL CONDITIONS:
      H$_2$O $\approx$ 0.68 MOLE %
      KF $\approx$ 1.0 MOLE %
      TEMP.=1-2°C
      INTERRUPTION RATE=1 SEC./120 SEC.

WITH POTENTIAL DECAY METHOD

WITH SQUARE WAVE METHOD

OF$_2$ YIELDS, % OF CURRENT

CURRENT DENSITY, AMPS/CM^2
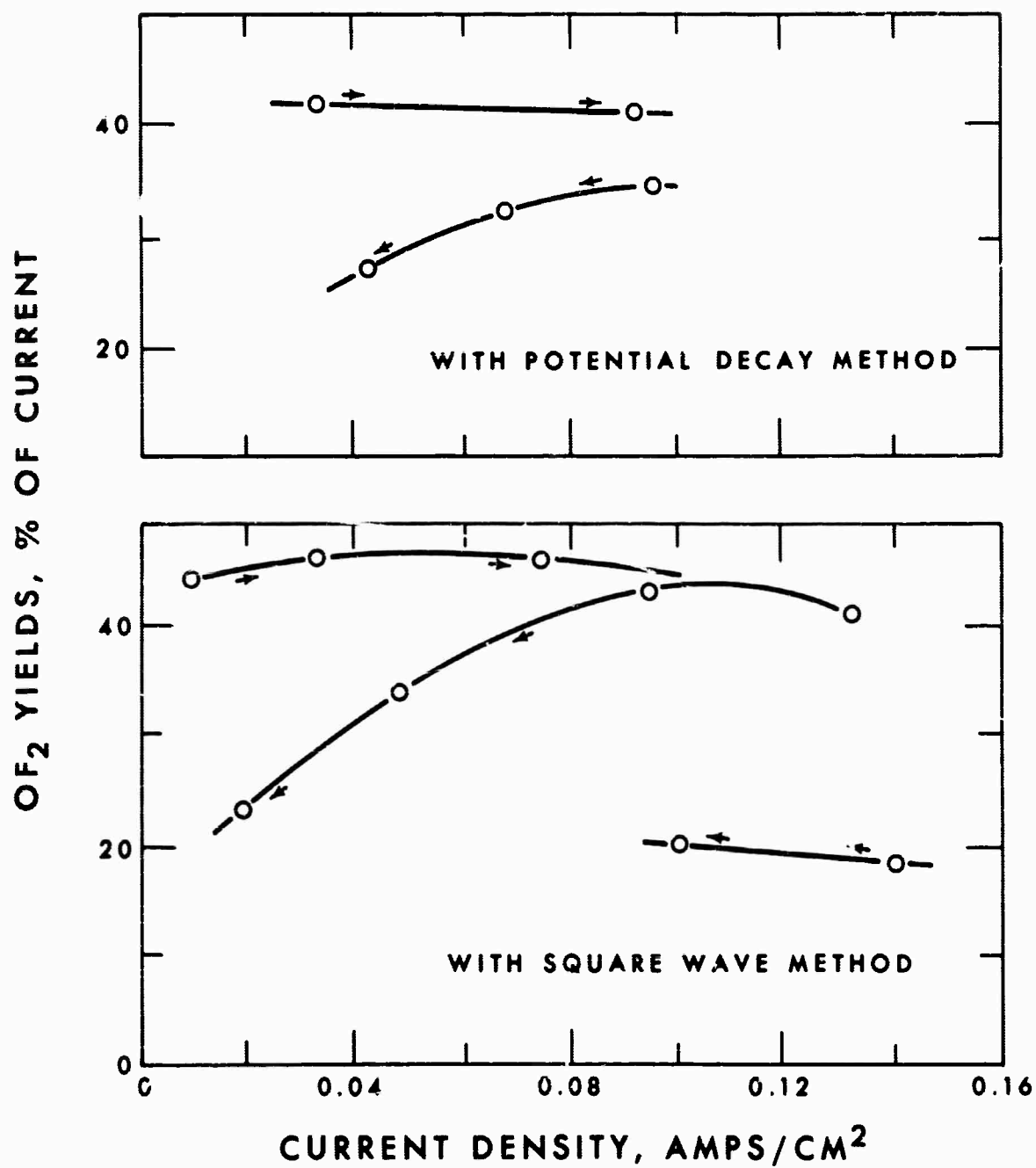
in both methods but was most pronounced in the square-wave method (lower half of Figure 6). This drop is not short-lived because measurements made a day later gave low OF_2 yields even at the higher current densities. But again the η_R's were unchanged. The anode η_R increases during the induction period at approximately the same rate as the current (Figure 7); hence, since $\eta_R = IR$, we find the resistance (R) of the anode film is constant during the induction period.

Limiting Potential ($E\infty$), Activation Overvoltage (η_A) and Concentration Overvoltage (η_C)--The optimum conditions for these determinations are still being studied. Thus far, $E\infty$ values vary over a 0.5 v. range (1.7 to 2.2 v.) with 2.0 v. average. Within this spread no correlation with CF_2 yields could be noted.

The $\eta_A + \eta_C$ had a wider range (2.5-3.5 v.) and appear to be the largest and probably the most important. Because the solution is well stirred by sparging and evolving gases, η_C should be small but not zero. Using the Hg/Hg_2F_2 electrode as a reference, Figure 8 shows an estimate of the components of cell voltage at a normal operating condition.

Oxygen Atom Reactions--Standard vacuum-line techniques with a Raytheon Microtherm unit were used to produce oxygen atoms. The behavior of nickel fluoride to O atoms is shown by the following equation:
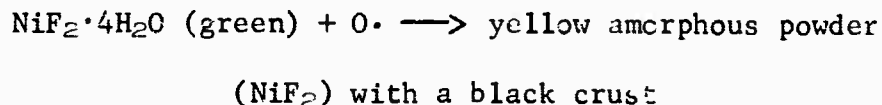
$$NiF_2 \cdot 4H_2O \text{ (green)} + O \cdot \longrightarrow \text{yellow amorphous powder}$$
$$(NiF_2) \text{ with a black crust}$$

FIGURE 7
INDUCTION PERIOD

CELL CONDITIONS:

$H_2O \approx 0.72$ MOLE %

$KF \approx 1.0$ MOLE %

TEMP. $= 1-2°C$

VOLTAGE-CONTROL $= 5.0$ V

CELL $= 6.2-6.5$

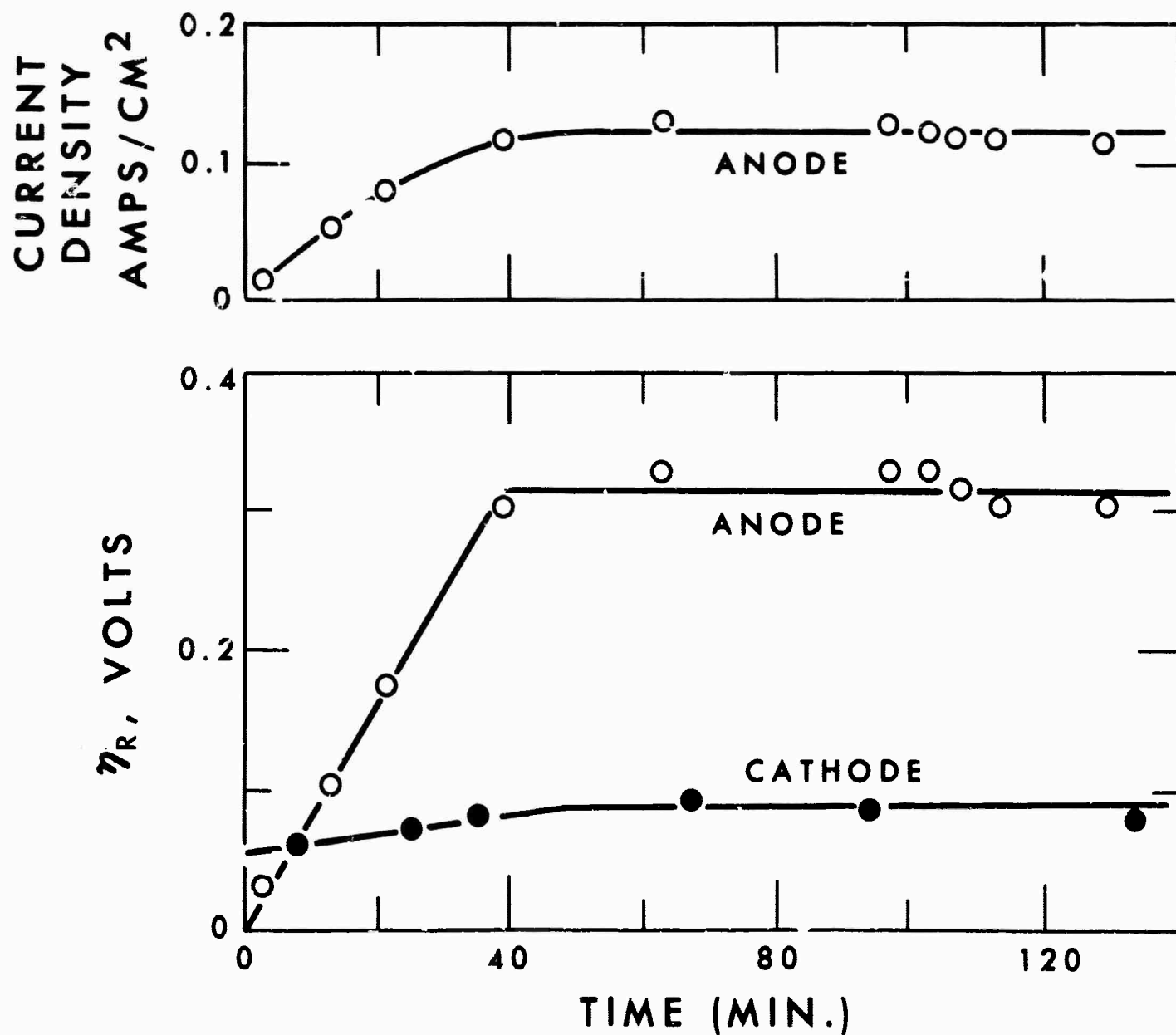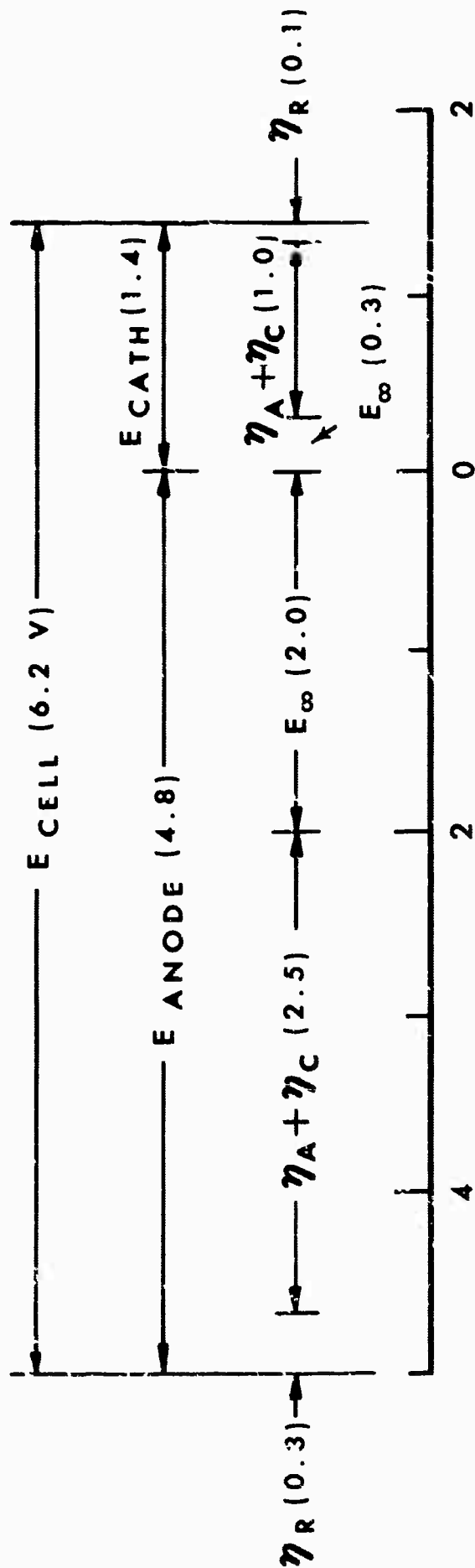INTERRUPTION RATE $= 1$ SEC./120 SEC.

FIGURE 8

COMPONENTS OF CELL VOLTAGE

$$E_\infty = E_0 + \frac{RT}{ZF} \ln \frac{(REACTANT)}{(PRODUCTS)}$$

The yellow powder is amorphous as it did not give an X-ray pattern. However, when $NiF_2 \cdot 4H_2O$ (B & A, Technical grade) was dried in an oven at 140°C, the resulting yellow powder was crystalline enough to show NiF_2 patterns. The black crust gave weak X-ray patterns that may be iron or chromium oxides, but no nickel oxide was detected. Possibly the Ni oxides are amorphous just as the yellow NiF_2.

Nickelic oxide (Baker C.P. analyzed) was reacted with 48% aqueous HF and with wet HF in the presence of KF as represented by the following equation:

$$\text{Nickel oxide} + HF \longrightarrow NiF_2 + H_2O + \text{gas}$$
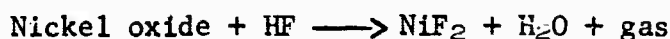
The gas from this reaction gave a positive KI test. However, when this gas was analyzed with the G.C. no OF_2 was found, and at most a trace of O_3, but there is an unidentified component.

None of these reactions give any definite support for our proposal that decomposition of H_2O gives oxygen atoms and these attack the $NiF_2 \cdot HF$ system to form OF_2.

Discussion

Voltage drop during interruption has no effect on OF_2 yield for intermediate values, but large drops seem to be beneficial. The present study did not examine very small voltage drops to determine how closely the actual operating potential can be approached before interruption becomes ineffective. Previous results indicate that suitable selection of interruption schedule can always raise OF_2 yield. Control of voltage drop during interruption may have a similar effect in permitting maximum OF_2 yields.

We expected the ohmic overvoltage at the anode to comprise a large portion of the anodic potential for two reasons: (1) nickel in HF is not attacked, presumably because of an impervious film; and (2) the large ohmic overvoltage observed during electrolysis of dry HF with nickel anodes has been attributed to anode film resistance.[8] However, we did observe that anode films in wet HF appeared thin and quite different from those in dry HF.[9] Furthermore, the current density was higher in wet HF. Apparently, the impervious anode film obtained during electrolysis of wet HF is a reasonably good conductor, or perhaps a semiconductor.

The much lower ohmic overvoltage in wet HF than in dry HF shows that water causes a large decrease in the anode film resistance. We do not know how the water affects the NiF_2 film. Formation of a hydrate ($NiF_2 \cdot 4H_2O$) is unlikely as it is dehydrated by anhydrous HF.[10] Our infrared reflectance spectra showed OH bonds and adsorbed water on an anode after use, but no special precautions were taken to prevent adsorption of moisture from the air after the anode was rinsed with HF and evacuated. We cannot be certain that absorptions in the infrared are due to material that survived contact with the electrolyte.

The unchanging resistance during the induction period and when OF_2 yields are different is surprising because we had assumed a marked change in the anode film. The nature of these changes will be investigated by other means.

Program

We plan to determine if products in the electrolyte contribute to the $E\infty$ of the potential decays and to an arrest in chronopotentiograms.[4] Using coulometry and chronopotentiometry, we will also study anode films during the induction period and after steady OF_2 yields have been attained at several levels.

IV. .IGH PRESSURE REACTIONS OF DIFLUORODIAZINE

During the last quarter we have made additional attempts to prepare $N_2F^+ClO_4^-$, have attempted to add F_2 to cis-N_2F_2, and have improved the procedure for isomerizing trans-N_2F_2 to cis-N_2F_2. Development of a capsule for use at very high pressures also was continued.

Further infrared studies of N_2F_2:SbF_5 complexes in SbF_5 solutions have failed to detect N-F stretches. However, an electron paramagnetic resonance examination of these solutions has revealed free radical species.

Preparation of $N_2F^+ClO_4^-$

Further attempts were made to form $N_2F^+ClO_4^-$ by the reactions of various combinations of NF_3, N_2F_2, and $Mg(ClO_4)_2$. At conditions of -78°C and 35,000 psig for 4 hours, no reaction took place with either a mixture of NF_3, cis-N_2F_2, and $Mg(ClO_4)_2$ in a mole ratio 7.5 to 1. In several attempts, mixtures of NF_3, cis-N_2F_2, and $Mg(ClO_4)_2$ in a mole ratio of approximately 10 to 4 to 1 ignited at about 0°C, and 50 to 83% of the cis-N_2F_2 decomposed. In contrast, mixtures of NF_3 and cis-N_2F_2 in a mole ratio of about 10 to 4 show only 20% decomposition of cis-N_2F_2 up to temperatures of 82°C. Apparently, the $Mg(ClO_4)_2$ either acts as a catalyst for the decomposition of cis-N_2F_2 or reacts first with NF_3. Why cis-N_2F_2 does not completely decompose on ignition is not known.

Addition of F_2 to cis-N_2F_2

All previous attempts to add to the N_2F_2 molecule to form liquids or solids have been unsuccessful. The addition of F_2 to N_2F_2

was not tried previously because the product would be a gas, N_2F_4. However, it was of interest to try this reaction in order to see if such an addition is possible. A 3 to 1 mole ratio of F_2 and cis-N_2F_2 was maintained at 87,000 psig and 69°C for 4 hours. No N_2F_4 was formed, but b.." of the cis-N_2F_2 decomposed. Apparently, F_2 is not as effective a diluent to prevent decomposition as NF_3 where only 20% decomposition occurred at 5 to 2 NF_3 to N_2F_2 at 82°C.

Isomerization of trans-N_2F_2

Isomerization of trans-N_2F_2 to cis-N_2F_2 was carried out in a stainless steel vessel for one hour at 75°C by a variation of Hurst's procedure.[11] Hurst activated bombs for the isomerization reaction by decomposing a small amount of trans-N_2F_2 in them. We have been unsuccessful in activating bombs in this way. Instead, we have found that isomerization will take place if a small amount of F_2 is mixed with the trans-N_2F_2. For example, when 150 mg of F_2 was added to 4 g of trans-N_2F_2, the yield of the cis isomer was about 94%, with a total recovery of 97%.

Very-High-Pressure Apparatus

We have continued evaluating capsules for use at very high pressures. Figure 9 shows a nickel capsule, fabricated in our shops, of semi-bellows design complete with valve. Figure 10 presents drawings of two electroformed nickel bellows with .002 and .010 wall thickness (Servometer Corporation, Clifton, N. J.). These bellows were joined to the internal valve and lower closure by silver soldering.
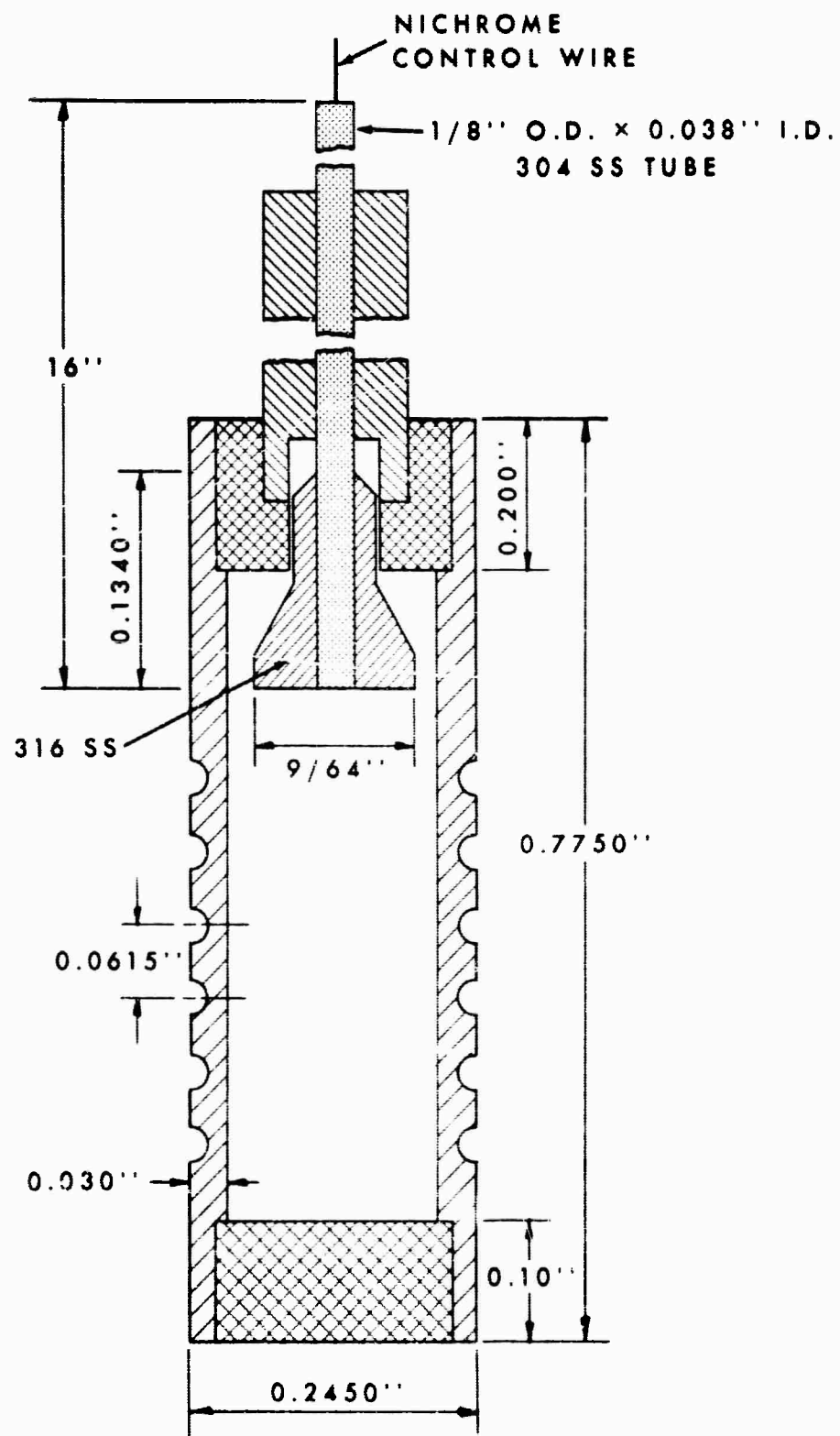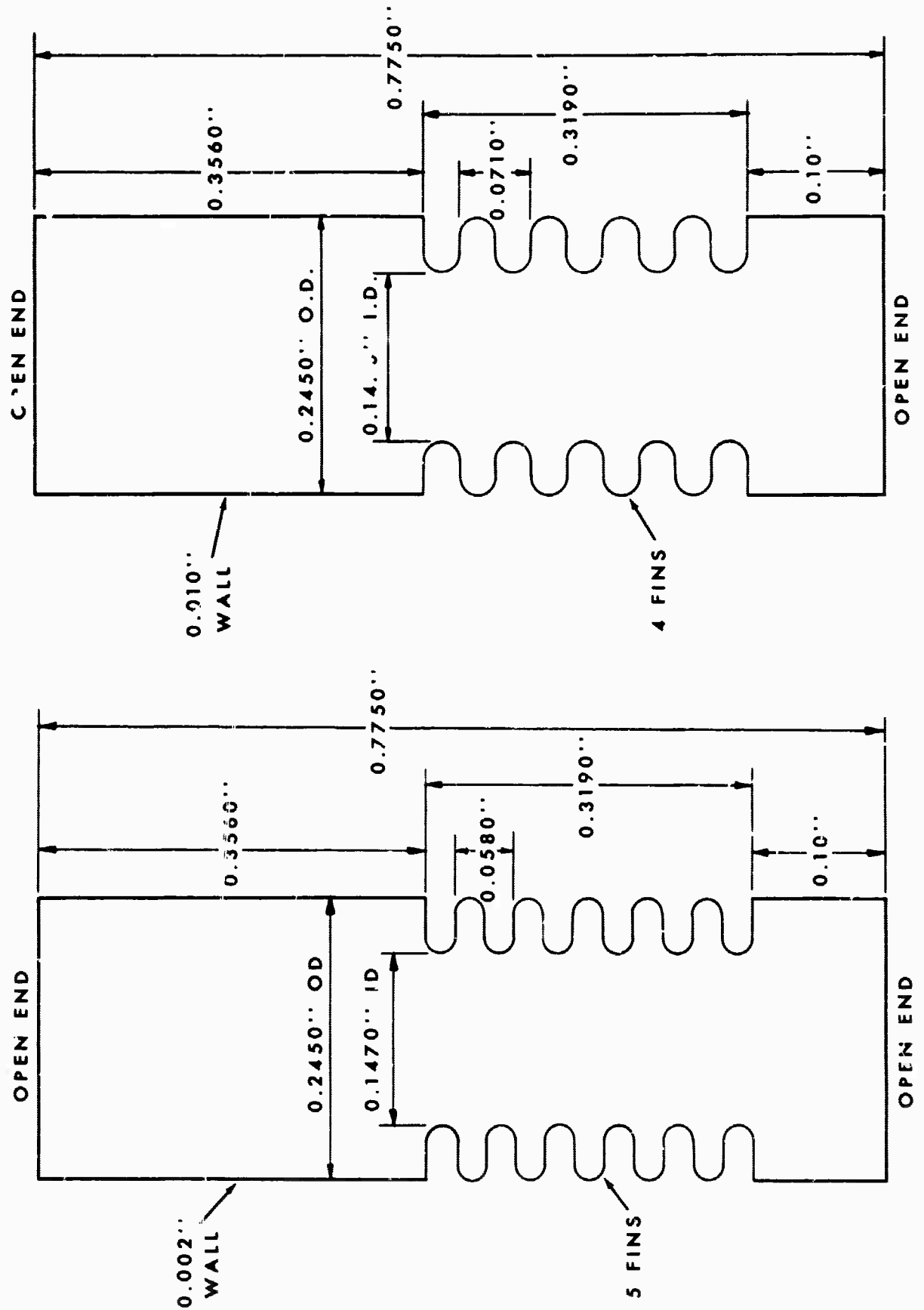
FIGURE 9
SEMI-BELLOWS TYPE NICKEL CAPSULE

FIGURE 10

ELECTRO-FORMED NICKEL BELLOWS

The capsule with semi-bellows was tested in the very-high-pressure apparatus with piston-cylinder device[4e] using ethane in the capsule. The capsule held until about 150,000 psi when the ethane was suddenly released. The internal valve was found to be deformed possibly due to squeezing by the cylinder walls of the device.

The piston-cylinder device was eliminated from the apparatus[4e] and tests were carried out hydrostatically. A capsule made from 0.002 inch thick bellows containing ethane was subjected to 50,000 psi. After depressuring the internal valve was opened and the ethane partially recovered. However, cracks were found in the recovered capsule; these probably occurred during ethane recovery and indicate the walls were too brittle.

A capsule made from a bellows with .010 inch wall was annealed before use. It was filled with liquid ethane and pressured hydrostatically to 125,000 psi. When pressure was dropped to atmospheric the internal valve could not be opened. However, when the capsule was removed from the pressure vessel and cooled in liquid nitrogen, the valve opened easily and the ethane was recovered. The walls of this capsule were intact.

In future experiments, attempts will be made to reach 200,000 psi and to pressure N_2F_2.

Infrared Study of N_2F_2:SbF_5

In preparing solutions of N_2F_2:SbF_5 in SbF_5, we observed a royal blue solution when N_2F_2 contacted the surface of the SbF_5. We are

attempting to obtain infrared spectra of this blue solution and the colorless or yellow solution from the N_2F_2:SbF_5 complex to determine whether a nitrogen-containing species such as N_2F^+ is present.

Our initial failure to detect N-F stretches at 1057 cm^{-1}, as found in solid state spectra, was attributed to inadequate mixing and sampling of the solution.[4] Therefore, the apparatus was modified so that the flow of SbF_5 and N_2F_2 into the Kel-F reaction tube could be alternated through a three-way valve[12] connected to Teflon tubing that extended to the bottom of the reaction tube. With this arrangement, a uniform blue solution was produced, and the color persisted so long as the N_2F_2 bubbled through the SbF_5. However, the solid complex eventually plugged the tubing and interrupted the flow. Nitrogen pressure was used to force the SbF_5 through the blockage and to force some of the solution into the infrared cell.[4g] The blue color disappeared before an infrared spectrum could be obtained. The resulting yellow solution failed to show N-F stretches.

To eliminate the plugging problem, the Teflon tubing was re-placed with a glass bubbler. With this arrangement, the SbF_5 was introduced through a Kel-F valve at the bottom of the bubbler, and the N_2F_2 was introduced through a tube at the top. Again, a uniform blue solution was produced, but it turned yellow a few seconds after bubbling of N_2F_2 was stopped, and no evidence for a N-F compound was found in its infrared spectrum.

EPR Study of N_2F_2:SbF_5

On the possibility that the blue color may indicate the presence of free radicals, the N_2F_2:SbF_5 solutions were examined by electron paramagnetic resonance. The solutions were prepared directly in the EPR cells in an apparatus similar to one that had been used for infrared studies.[4f] The cells were of two types. The first was 1/4-in. O.D. Kel-F tubing heat-sealed at the bottom. It was not satisfactory because it would not hold SbF_5 for more than one hour before a hole developed. The second, shown in Figure 11, was pyrex glass. Spectra were obtained on a modified Varian Model V4500 spectrometer operated at x-band frequencies of about 9500 mc/sec. For increased sensitivity, a Varian Model V4560 100-kc Modulating Unit was used. The rectangular cavity operated in the TE_{012} mode. The cavity is actually a low-loss tuneable short. Such an adjustable wave-guide short is of the non-contracting type for minimum r-f loss.

Figure 12 shows blank EPR spectra for: (a) the empty Kel-F cell, (b) the empty glass cell, and (c) freshly distilled SbF_5 in the glass cell. No signal is apparent in the Kel-F spectra, but a weak signal is evident in the other two.

Figures 13 and 14 show the spectra for the yellow N_2F_2:SbF_5 solution in Kel-F and in glass. The sample in Kel-F shows two distinct species--at g = 2.002 and 2.027--whereas the sample in glass shows only one--at g = 2.027. To test whether Kel-F was contributing to the spectrum, Kel-F particles were added to a glass tube before the N_2F_2:SbF_5 was added. The EPR spectrum of this sample is shown in Figure 15. Two species are
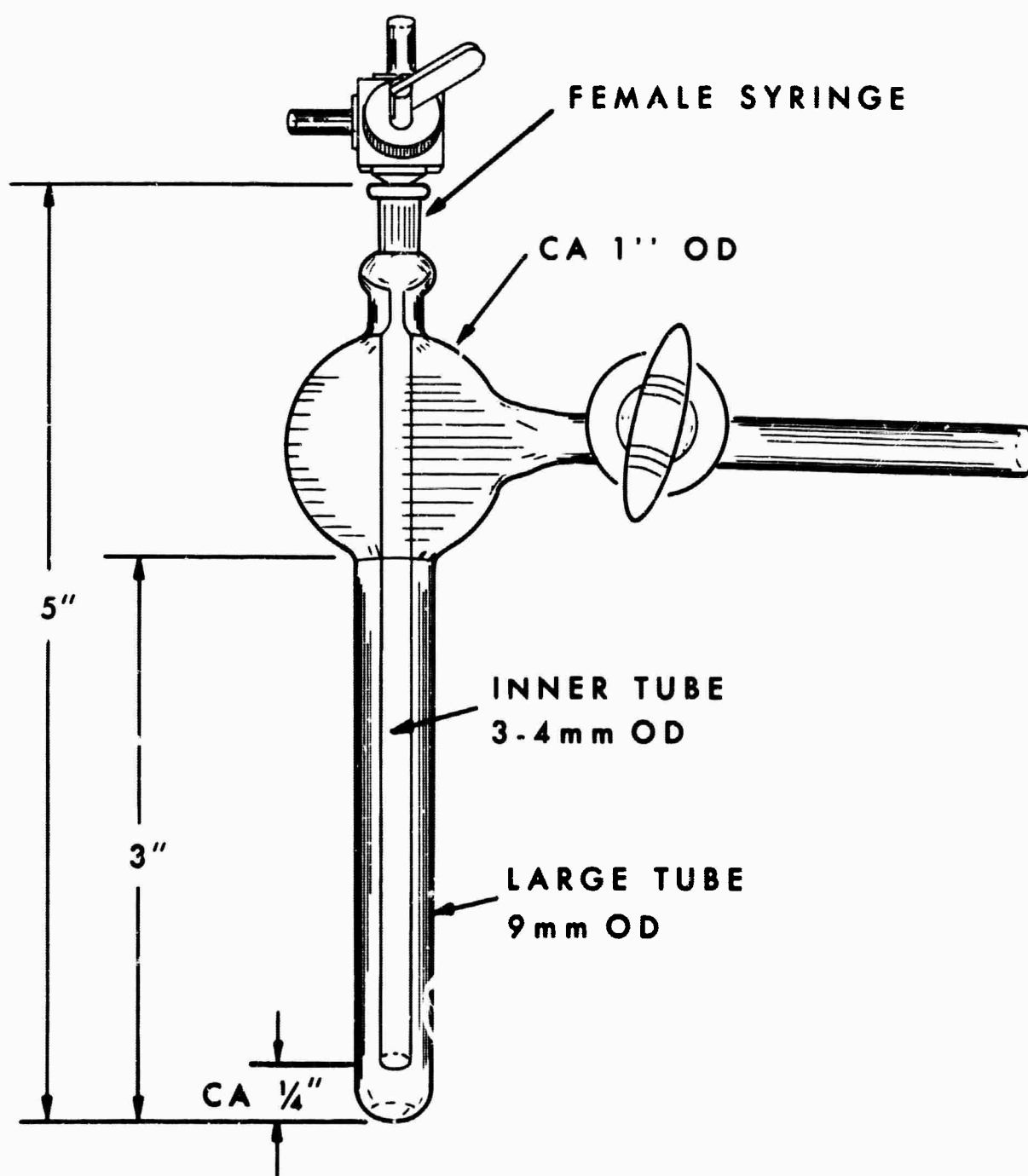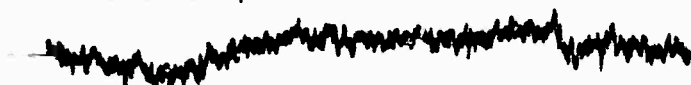
FIGURE 11

GLASS CELL FOR EPR STUDIES

FEMALE SYRINGE

CA 1'' OD

INNER TUBE
3-4mm OD

LARGE TUBE
9mm OD

5"

3"

CA ¼"

FIGURE 12
BLANK EXPERIMENTS

a. KEL F TUBING
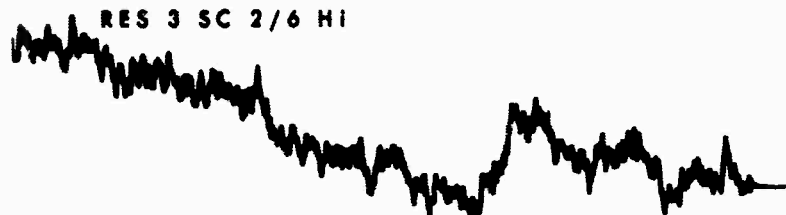
S-8×100
M-4×100
RES 2 SC 2/4

|
3460.0

|
3675.0

b. PYREX GLASS TUBE

S-2×1000
M-4×100
RES 3 SC 2/6 Hi

|
3050.0

|
3820.0

c. DISTILLED SbF$_5$ IN GLASS TUBE

S-2×1000
M-4×100
RES 3 SC 2/6 Hi

|
3050.0

|
3820.0

GAUSS

FIGURE 13
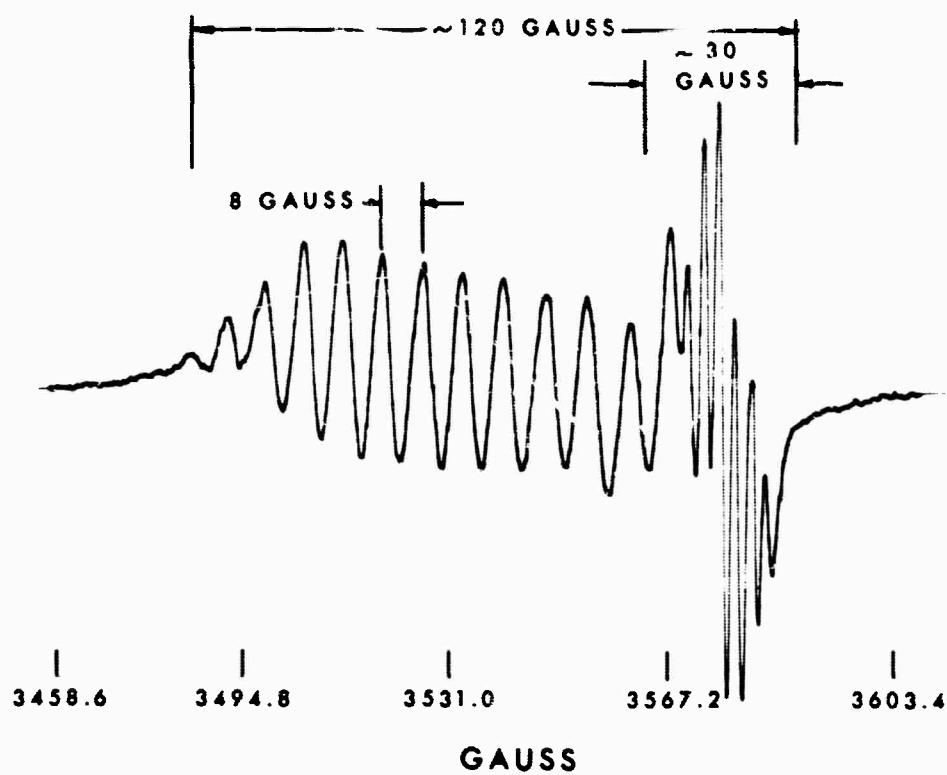## EPR SPECTRUM OF CIS-N₂F₂-SbF₅ SOLUTION IN KEL-F

GAUSS

FIGURE 14
EPR SPECTRUM OF
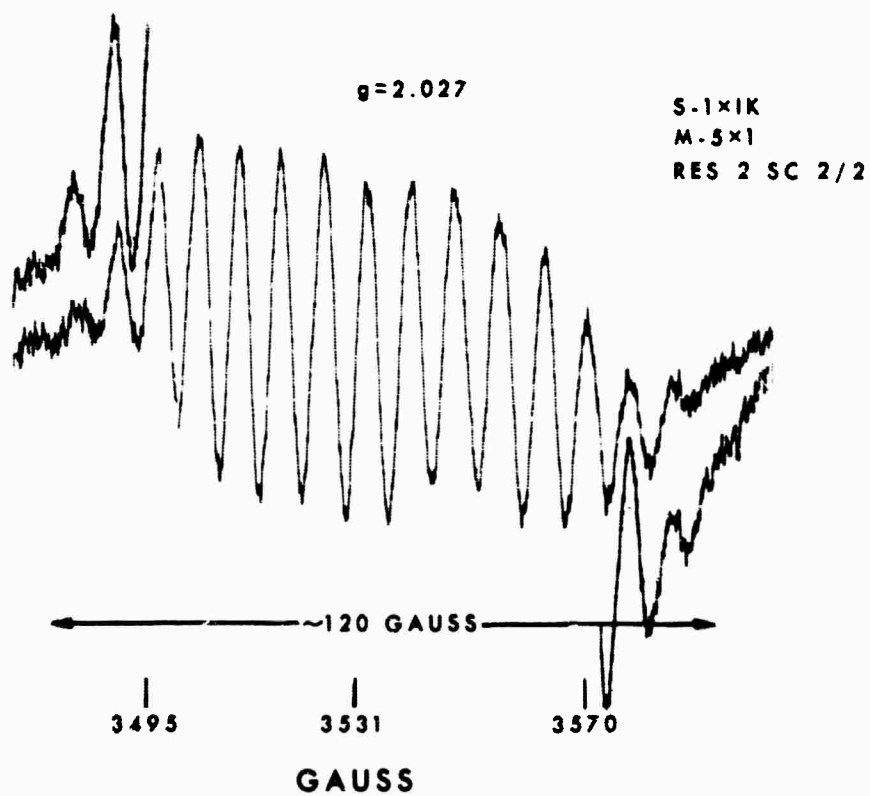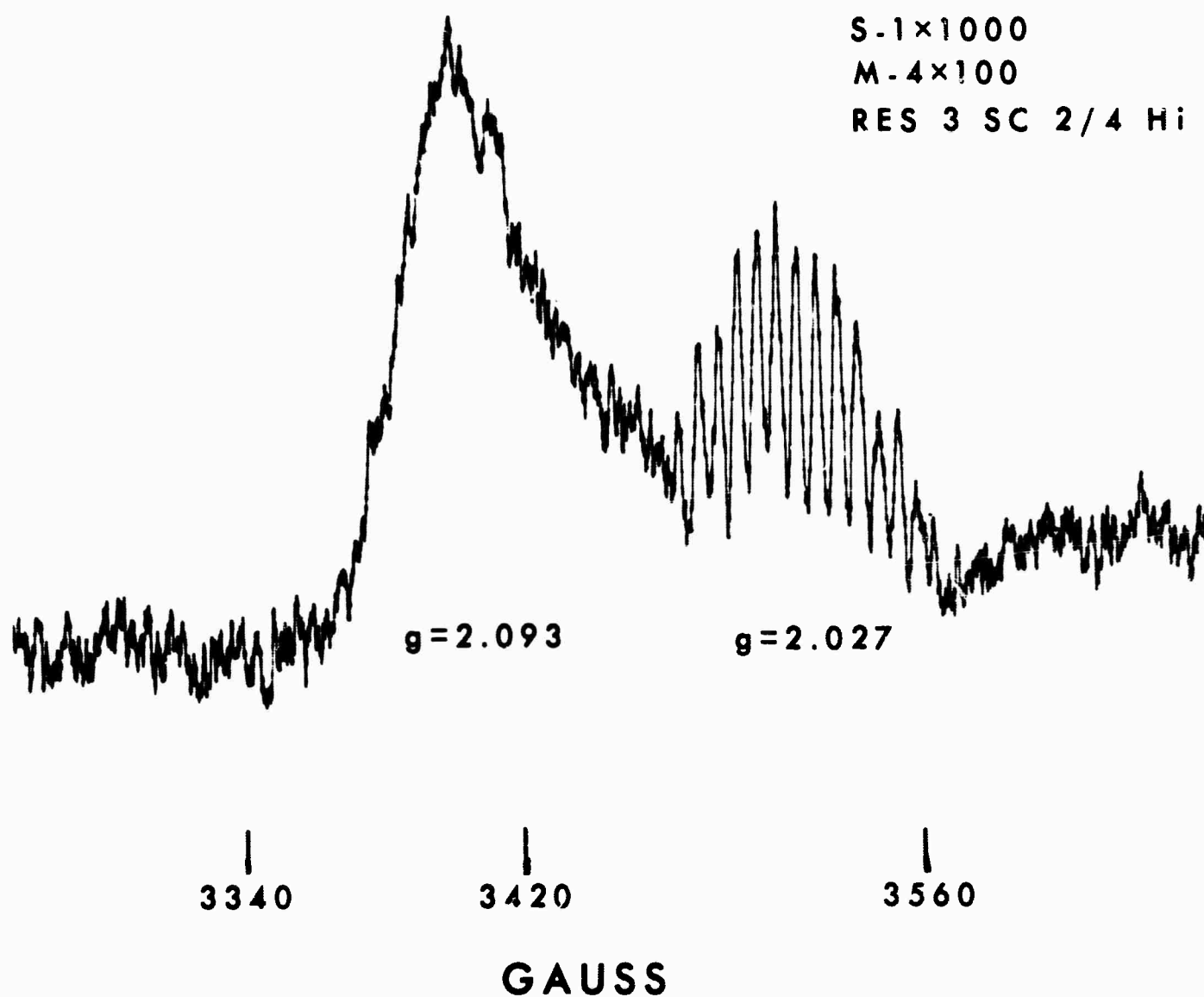## CIS-N₂F₂-SbF₅ SOLUTION IN GLASS

GAUSS

FIGURE 15

EPR SPECTRUM OF CIS-N_2F_2-SbF_5 SOLUTION IN GLASS CONTAINING KEL-F

evident, but only the one at g = 2.027 corresponds to the spectrum of $N_2F_2:SbF_5$ in glass; the other represents a new species at g = 2.093.

The spectrum in Figure 13 can be resolved into two separate spectra, as shown by the hand drawings in Figure 16. The five-line spectrum is consistent with an N_2 containing radical in which the ^{14}N atoms, with nuclear spin (I) of one, give rise to the splitting:

$2I_{Total} + 1 = 2 \times 2 + 1 = 5$.

The splitting and the expected intensities are diagrammed in Figure 17. The five-line spectrum exhibits the same intensity pattern. Furthermore, the g-value of 2.002 is consistent with a nitrogen-containing radical, and the overall band width of about 30 gauss is compatible with ^{14}N splittings. However, the number of bonded fluorines cannot be ascertained from these spectra but may be revealed if fine structure EPR spectra can be obtained, showing the ^{19}F splittings. Absence of the N_2 radical signal in glass (Figure 14) may be due to adsorption.

The 16-line spectrum in Figure 16 was extracted from Figure 13 with the aid of the spectrum in glass in Figure 14. The g-value is 2.027 and the band width is about 120 gauss. Evidence shows it arises from an antimony-containing radical. The g-value coincides with that of the six-line spectrum ($I_{121Sb} = 5/2$) of the paramagnetic sites in powdered Sb_2S_5, as shown in Figure 18. The band width is similar to that found in aqueous $NO^+SbF_6^-$ (Figure 19) and $SbCl_3$ in acetone (Figure 20).

Spin-spin coupling constants for antimony are chosen to be 16, 24 or 32 gauss to fit the observed band width, while that for ^{19}F is

FIGURE 16
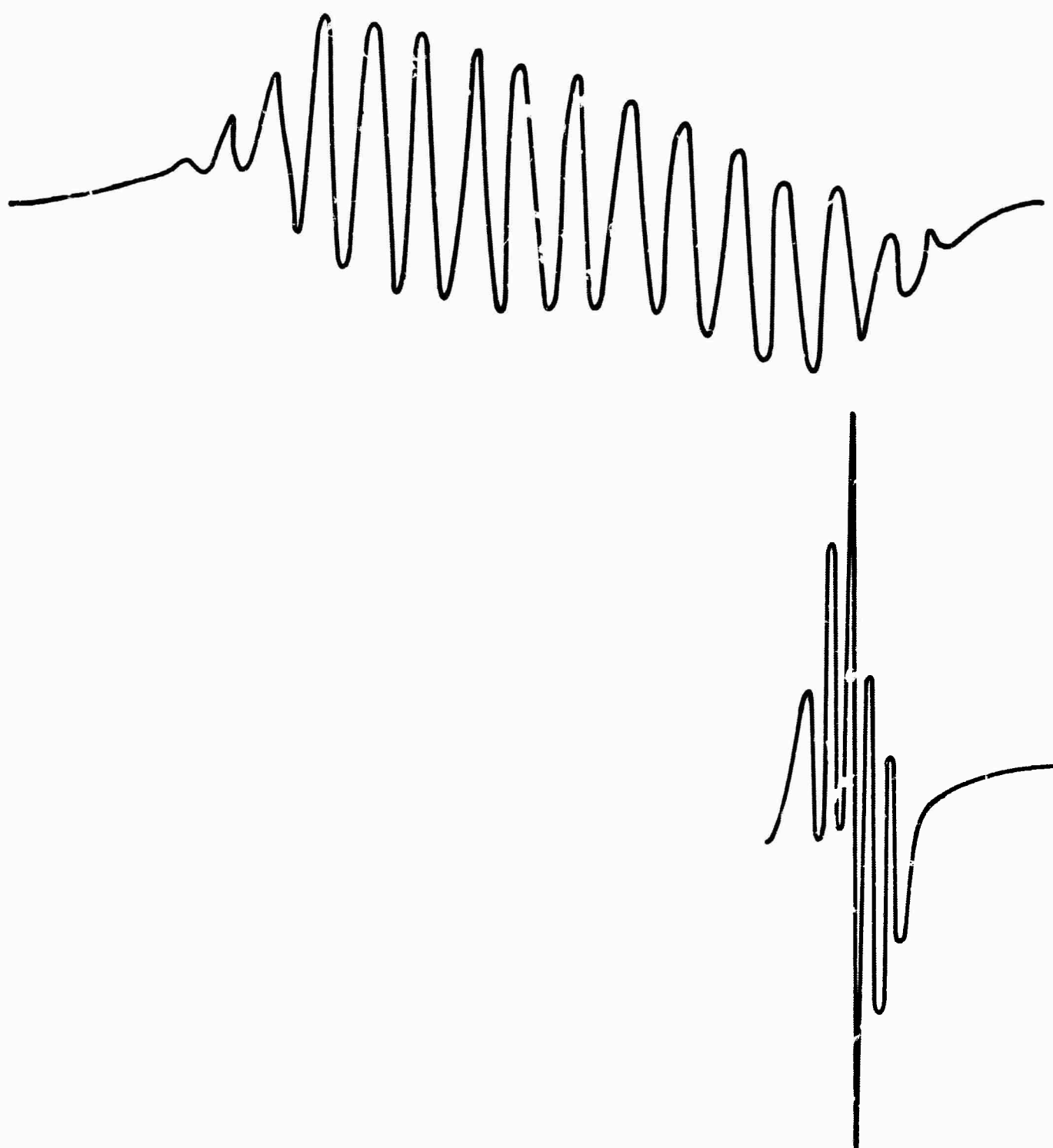
RESOLUTION OF EPR SPECTRUM IN KEL-F
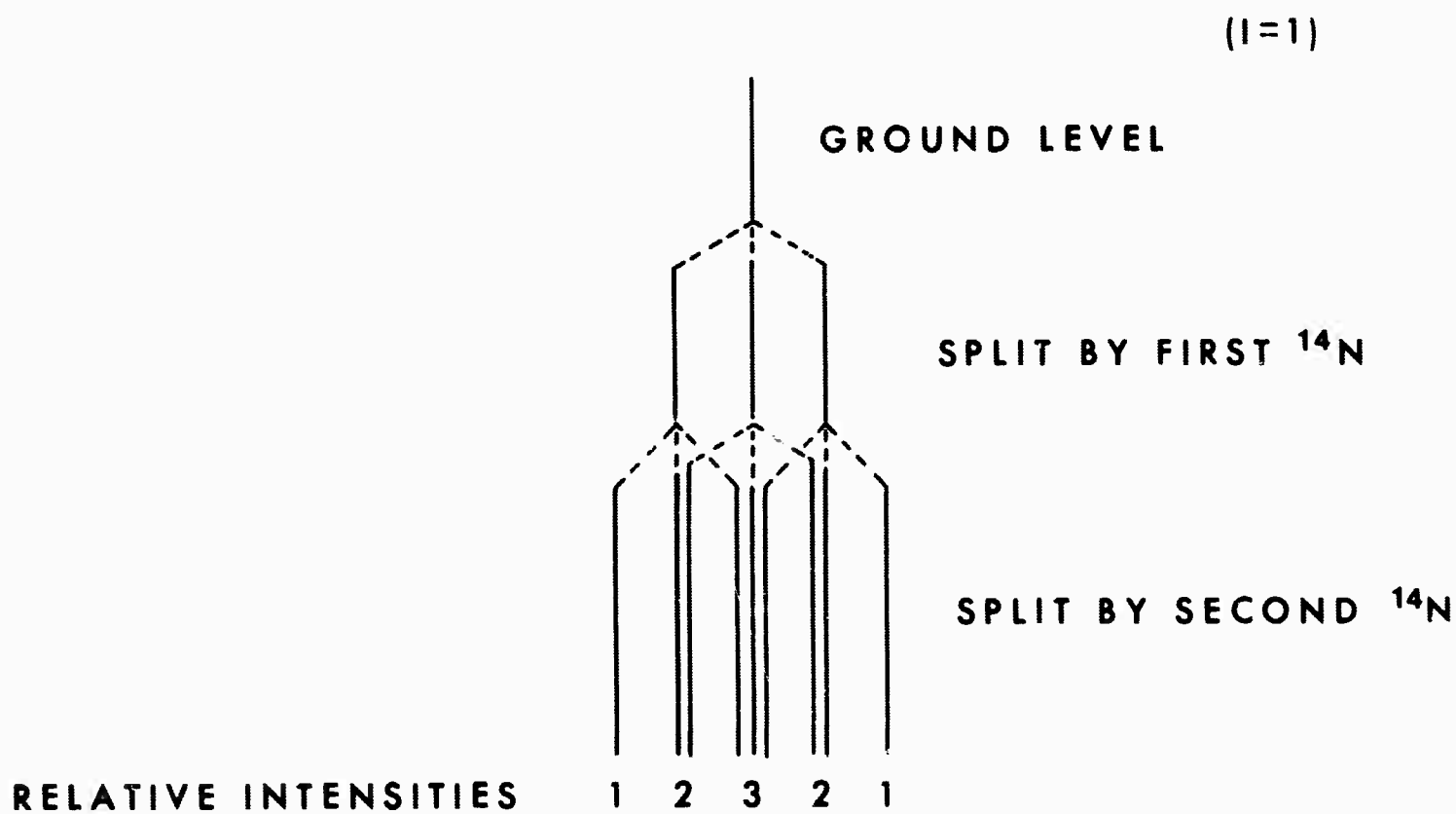
FIGURE 17

SPLITTING DIAGRAM FOR N_2 RADICAL SPECIES

$(I=1)$

GROUND LEVEL

SPLIT BY FIRST ^{14}N

SPLIT BY SECOND ^{14}N

RELATIVE INTENSITIES   1   2   3   2   1

- 42 -

FIGURE 18

EPR SPECTRUM OF SOLID ANTIMONY PENTASULFIDE

S-2×IK
M-4×10C
RES 3 SC 2/6 Hi

g=2.021

3820
GAUSS

3250
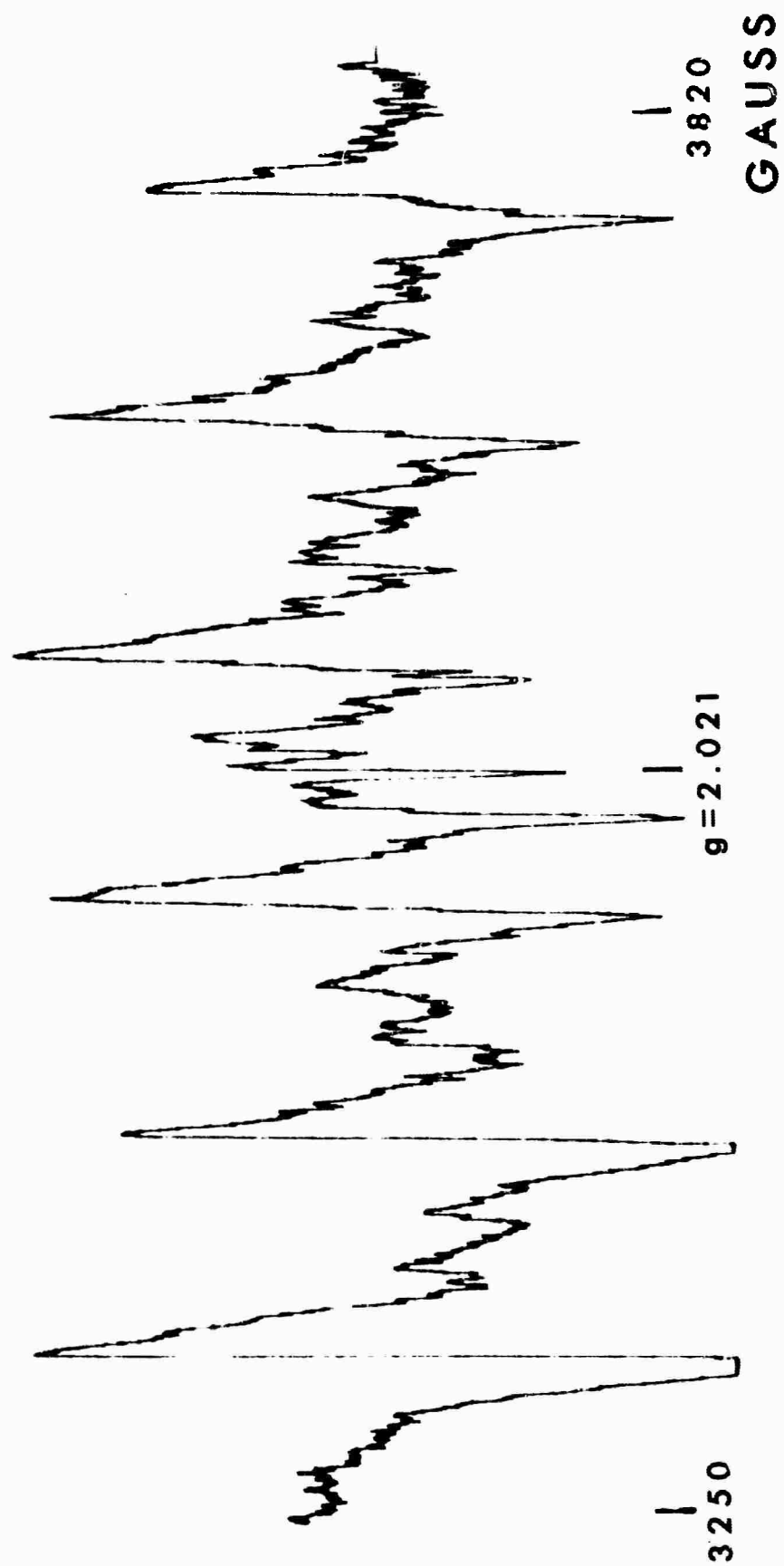
FIGURE 19
EPR SPECTRUM OF NO$^+$SbF$_6^-$ IN WATER

1 DAY LATER   S-2×1K
ALSO ADDED   M-4×100
MORE H$_2$O   RES 3 SC 2/6 Hi

~100 GAUSS

3040   3420
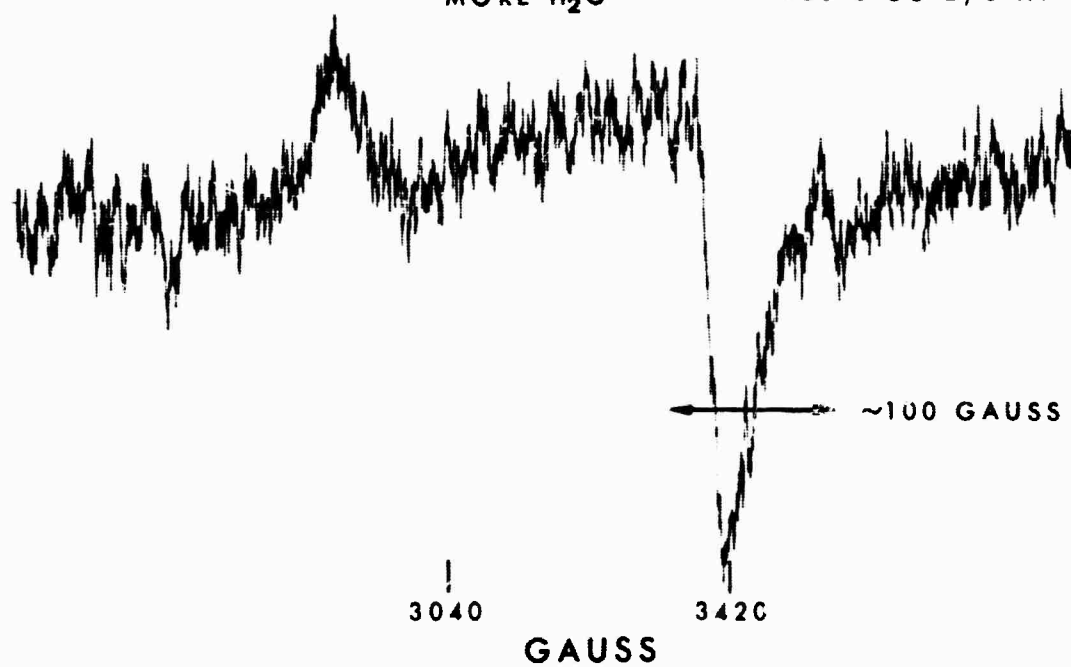
GAUSS

FIGURE 20
EPR SPECTRUM OF SbCl$_3$IN ACETONE

S-2×1K
M-4×100
RES 3 SC 2/5 Hi

~100 GAUSS

3040   3420
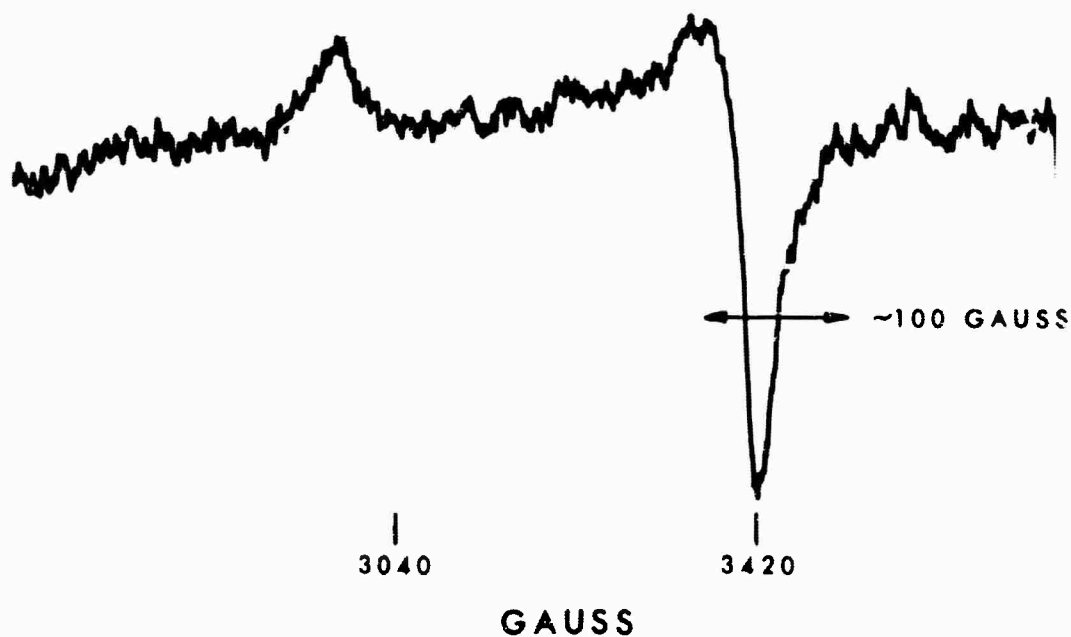
GAUSS

about 8 gauss.[13] Several antimony fluoride species are possible, such as SbF_4, SbF_5^-, SbF_6, or SbF_6^{2-} free radicals. The combinations of antimony and fluorine spin-spin couplings for each structure as shown in Figure 21. The constructed spectrum for SbF_5^-, using the Sb coupling constant of approximately 16, fits the observed spectrum very closely in predicted splittings (16 lines total) and intensities (Figure 22). In Figure 22, and even more so in Figure 14, the lack of symmetry with respect to the center of the pattern is evident. This phenomenon apparently arises from anisotropy of the radical species interacting with the nuclear orientations possible in the external field[14], and is consistent with the trigonal bipyramide structure for SbF_5. The lack of fit of the spectrum with SbF_6 appears to exclude the location of the electron on an Sb atom of the linear chain structure attributed to liquid SbF_5.[15] Perhaps addition of an electron to the Sb in such a chain frees that SbF_5 unit.

The presence of SbF_5^- as the counter species to the N_2 radical species suggests a single electron transfer:

$$N_2F_2 + SbF_5(soln) \longrightarrow N_2F_2^+SbF_5^-(soln)$$
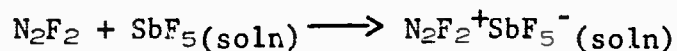
However, that the N_2 species arises from N_2F_2 rather than from an impurity, such as N_2O or N_2O_2, has to be varified.

Program

We will continue attempts to add to N_2F_2 at high pressure and will attempt to pressure N_2F_2 to near 200,000 psi. Infrared and EPR studies of N_2F_2 solutions in SbF_5 will be continued.

FIGURE 21

SPLITTING DIAGRAMS FOR ANTIMONY FLOURIDE RADICAL SPECIES

(HALF OF SPECTRAM SHOWN)

FIGURE 22

COMPARISON OF CALCULATED AND
OBSERVED SPECTRUM FOR SbF_5^-
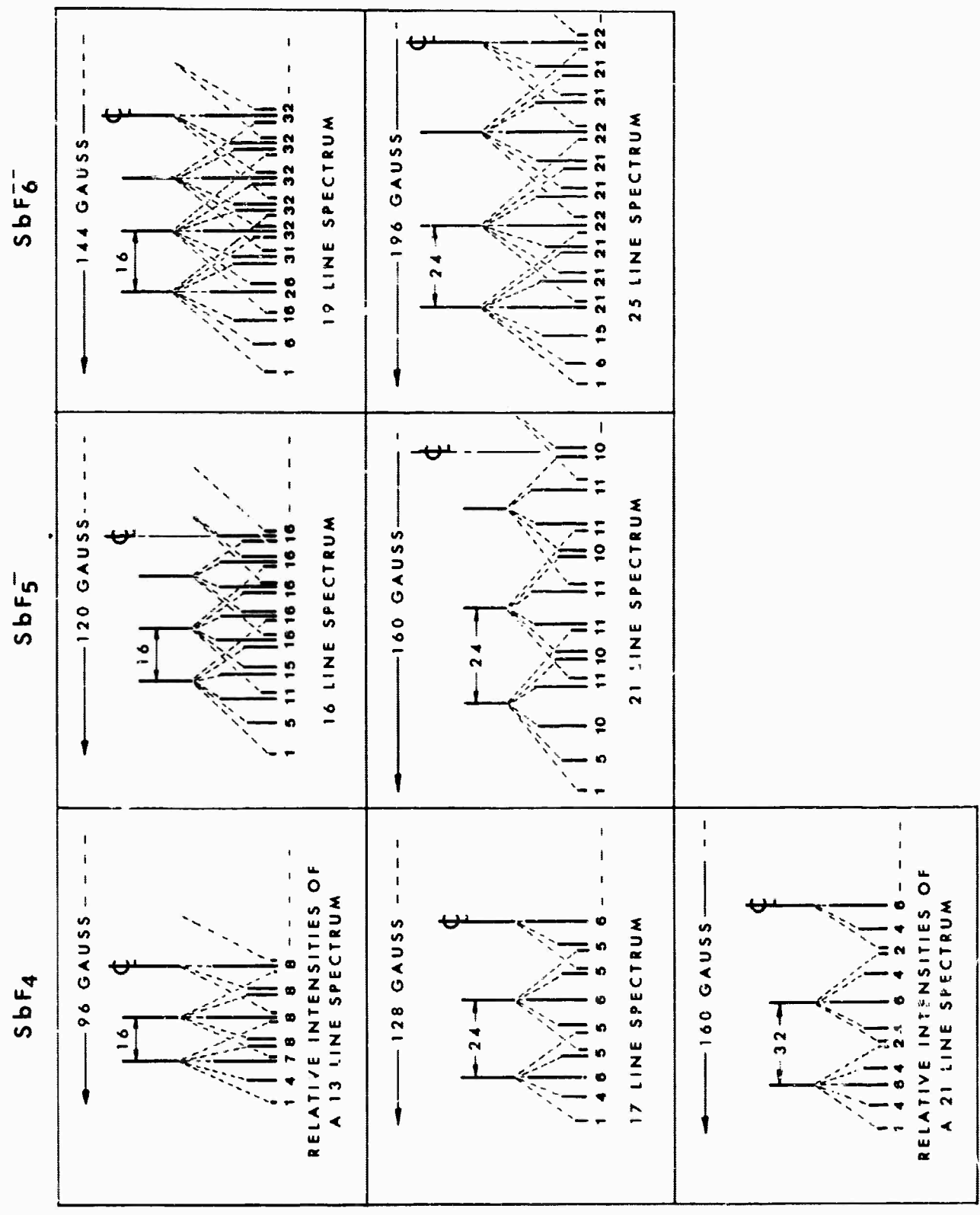
V. REFERENCES

1. A. Arkell, R. R. Reinhard and L. P. Larson, J. Am. Chem. Soc. 87, 1016 (1965).

2. Second Annual Report, this contract: (a) pp. 44 and A-9; (b) pp. A-10 and A-14.

3. Ninth Quarter Report, this contract.

4. Tenth Quarter Report, this contract: (a) p. 5; (b) p. 6; (c) p. 17; (d) p. 25; (e) Figure 13; (f) Figure 10; (g) Figure 11.

5. R. D. Stewart and G. H. Cady, J. Am. Chem. Soc. 77, 6110 (1955).

6. G. H. Cady and K. B. Kellogg, J. Am. Chem. Soc. 75, 2501 (1953); G. L. Gard and G. H. Cady, Inorg. Chem. 4, 594 (1965).

7. P. B. Ayscough and E. W. R. Steacie, Proc. Roy. Soc. A234, 476 (1956).

8. A. J. Arvia and J. Bebczuk de Cusminsky, Trans. Faraday Soc. 58, 1019 (1962).

9. First Annual Report, this contract.

10. A. F. Clifford and A. C. Tulumello, J. Chem. Eng. Data, 8, 425 (1963).

11. G. L. Hurst and S. I. Khayat, "Investigation of the Existence of Oxyanions of Fluorine and Nitrogen and the Nitrogen-Fluorine Cations," Quarterly Technical Summary Report No. HQ-76-9, May 28, 1965, ARPA Order No. 402, Program Code No. 3910, The Harshaw Chemical Company.

12. Hamilton Company, Whittier, California.

13. A. H. Maki and D. H. Geske, J. Am. Chem. Soc. 83, 1852 (1961).

14. G. E. Pake, Paramagnetic Resonance, W. A. Benjamin, Inc., New York, p. 110 (1962).

15. C. J. Hoffman, B. E. Holder, and W. L. Jolly, J. Phys. Chem. 62, 364 (1958).